Review of Palaeobotany and Palynology 216 (2015) 101–122

Contents lists available at ScienceDirect

Review of Palaeobotany and Palynology

journal homepage: www.elsevier.com/locate/revpalbo

Review papers

Palynofacies and geochemical analysis of Oligo-Miocene bituminous rocks from the Moldavidian Domain (Eastern Carpathians, Romania): Implications for petroleum exploration

Daniel Ţabără [a,*], Muriel Pacton [b,c], Matthew Makou [b], Gabriel Chirilă [a,d]

[a] "Al. I. Cuza" University of Iaşi, Department of Geology, 20A Carol I Blvd., 700505 Iaşi, Romania
[b] Laboratoire de Géologie de Lyon: Terre, Planètes, Environnement (UMR 5276 CNRS), Université Claude Bernard - Lyon 1, 69622 Villeurbanne, France
[c] ETH Zürich, Geological Institute, Sonneggstrasse 5, 8092 Zürich, Switzerland
[d] Halliburton Energy Services Romania, Şerban Vodă Street, no. 133, District 4, Bucharest, Romania

ARTICLE INFO

Article history:
Received 16 July 2013
Received in revised form 22 January 2015
Accepted 14 February 2015
Available online 24 February 2015

Keywords:
Palynology
Palynofacies
Organic geochemistry
Oligo-Miocene
Eastern Carpathians

ABSTRACT

A palynological, palynofacies and geochemical investigation conducted on Oligo-Miocene bituminous rocks of the Lower Dysodilic Shale Formation and the Upper Dysodilic Shale Formation (Eastern Carpathians) has allowed recovery of pollen and spore assemblages associated with marine palynofossils (dinoflagellates and prasinophyte algae) and phytoclasts. The general composition of the assemblages suggests an anoxic depositional environment from a distal basin to a highly proximal shelf. The palynological assemblage identified in the Lower Dysodilic Shale Formation exhibits an abundance of dinoflagellate cysts and prasinophyte algae, with some taxa, such as *Wetzeliella gochtii*, *Rhombodinium draco* and *Cordosphaeridium gracile*, indicating a Rupelian–early Chattian age for these deposits. In contrast, the Upper Dysodilic Shale Formation displays diverse assemblages of palynomorphs (more pollen and spores) and its age is older than middle Aquitanian. Geochemical (Total Organic Carbon content and Rock-Eval pyrolysis) and palynofacies (optical and scanning electron microscopy) analyses performed on samples from the Lower Dysodilic Shale Formation suggest that it contains type II kerogen (oil prone), consisting of abundant amorphous organic matter (AOM), extracellular polymeric substances (EPS) and coccoid bodies (bacteria or algae). This kerogen comes from a marine source (derived from phytoplankton and bacteria), and likely accumulated in a distal suboxic-anoxic basin. The Total Organic Carbon (TOC) content suggests good to excellent petroleum potential, especially for generating mixed oil and gas. The level of kerogen maturation (inferred from the Thermal Alteration Index, T_{max} and prasinophyte algae fluorescence) lies at the boundary between immature and mature phases. The Upper Dysodilic Shale Formation is abundant in translucent and opaque phytoclasts, suggesting a continental organic matter source and type III kerogen, and thus would yield mainly gas. This organic matter was principally deposited in a highly proximal shelf setting.

Contents

* Corresponding author. Tel.: +40 232 201469.
E-mail address: dan.tabara@yahoo.com (D. Ţabără).

http://dx.doi.org/10.1016/j.revpalbo.2015.02.002
0034-6667/

1. Introduction

The main types of bituminous rocks in the Eastern Carpathian region are menilites, brown marls and the bituminous shale belonging to the Tarcău and Vrancea Nappes. These rocks, which have a high content of organic matter, were formed under anoxic conditions in the sedimentary basin that occurred along the Carpathian Chain during the Oligocene. Their organic content in relation to oil production and degree of maturity have been documented by Nacu et al. (1970), Balteş (1983), Stănescu and Morariu (1986), Grasu and Catană (1989), Ştefănescu et al. (2006) and Grasu et al. (2007). Based on geochemical studies (TOC amounts and Rock-Eval parameters), recent papers (Belayouni et al., 2009; Amadori et al., 2012) have shown that the bituminous rocks from this area can be regarded as having good petroleum potential, being in a sub-mature to mature thermal stage, and generally containing type II kerogen (lipidic organic matter, good oil and gas-prone source rocks). The present study focuses on the analysis (optical and geochemical) of organic matter from Oligocene–Miocene bituminous rocks, in an attempt to provide new data regarding the palynofacies, palynological assemblages and hydrocarbon potential of these formations. It is the first detailed description of the optical appearance in transmitted light microscopy and scanning electron microscopy (SEM) of the organic matter contained in the main hydrocarbon source rocks from the Eastern Carpathian Flysch zone.

The aims of the present study are thus the following: (1) identify palynological taxa (derived from either terrestrial or marine environments), and reconstruct palaeoecological conditions; (2) use the assemblages for biostratigraphic age assignment and correlation; (3) analyze the palynofacies characteristics of the sedimentary formations studied, using various microscopic techniques; (4) determine the source rock potential for hydrocarbons generation based on geochemical analyses; and (5) identify the different kerogen types and determine their thermal maturity.

2. Geological settings

The Carpathian Chain in Romania resulted from a collision between the African–Arabic and European plates, which led to the gradual closure of the Tethys Ocean during the Cretaceous and Miocene convergence events (Săndulescu, 1984). According to Săndulescu (1984), the deformation in the Romanian Carpathians took place in two stages: (a) — in the Cretaceous period, when the Transylvanide and Dacide Units were built up; (b) — during the Miocene, when the Moldavidian Unit in the Eastern Carpathians was formed. The Moldavidian Unit includes, from west to east, the following tectonic nappes: Teleajen, Macla, Audia, Tarcău, Vrancea and the Pericarpathian Nappe (Fig. 1).

The Paleogene–Miocene deposits included in various structural units of the Moldavide sometimes display considerable lateral facies variation. Thus, three distinct lithofacies have been identified (Băncilă, 1958; Ionesi, 1971) in the Tarcău Nappe: the Fusaru Lithofacies in the west, Moldoviţa Lithofacies (mixed) in the center, and the Kliwa Lithofacies in the eastern part. In the lithological profiles analyzed from Tarcău Nappe, the samples were collected only from the Kliwa Lithofacies (Fig. 1).

The Kliwa Lithofacies sedimentary deposits consist of quartzarenites (of the Kliwa type), composed of mineral particles with a possible external (cratonic) source. In the case of the bituminous rocks (of Oligocene–early Miocene age), the sediment consist mainly of pelitic, bituminous marls and black shales that are generally silty-clayey, and menilites containing a silicious material. These were deposited under anoxic conditions, which enhanced organic matter preservation. This organic matter is considered to be autochthonous (marine); its accumulation being uniform throughout the External Flysch basin (Grasu et al., 2007).

In the Kliwa Lithofacies, the limit of erosion reached the Kliwa Formation, while newer sedimentary deposits than this can be identified in the Vrancea Nappe, and are assigned to the Upper Dysodilic Shale and Gura Şoimului Formations (Fig. 1).

In the Eastern part of the Kliwa Lithofacies, corresponding to the Tarcău Nappe, a second lithofacies (named Pietricica) included in the Vrancea Nappe, was identified. This nappe is structurally interposed between the Tarcău and Pericarpathian Nappes, and is found below the Tarcău Nappe (Fig. 1 — Geological section). It occurs in outcrops as a tectonic window or as half-windows, resulting from erosion of the covering nappe (Fig. 1). Stratigraphically, the deposits assigned to the Vrancea Nappe are of Senonian, Paleogene and early Miocene age (Ionesi, 1971; Grasu et al., 1988). These deposits are generally similar to those of the Kliwa Lithofacies. However, there are certain differences, such as the reduction in thickness of the Kliwa Formation or the appearance of ruditic facies with “green schists” of the Central Dobrogea type (Ionesi, 1971; Grasu et al., 1999).

Fig. 1. Geological map with the locations of the stratigraphic sections studied (noted LS1–LS5). Geological cross-section according to Bădescu (2005). Lithological column according to Grasu et al. (2007). Geological maps: A. Humor Half-window (after Ionesi, 1971), B. Bran-Dumesnic tectonic window (after Grasu et al., 1976), C. Bistriţa Half-window (Micu, 1976), D. Slănic-Oituz Half-window (after Dumitrescu et al., 1968).

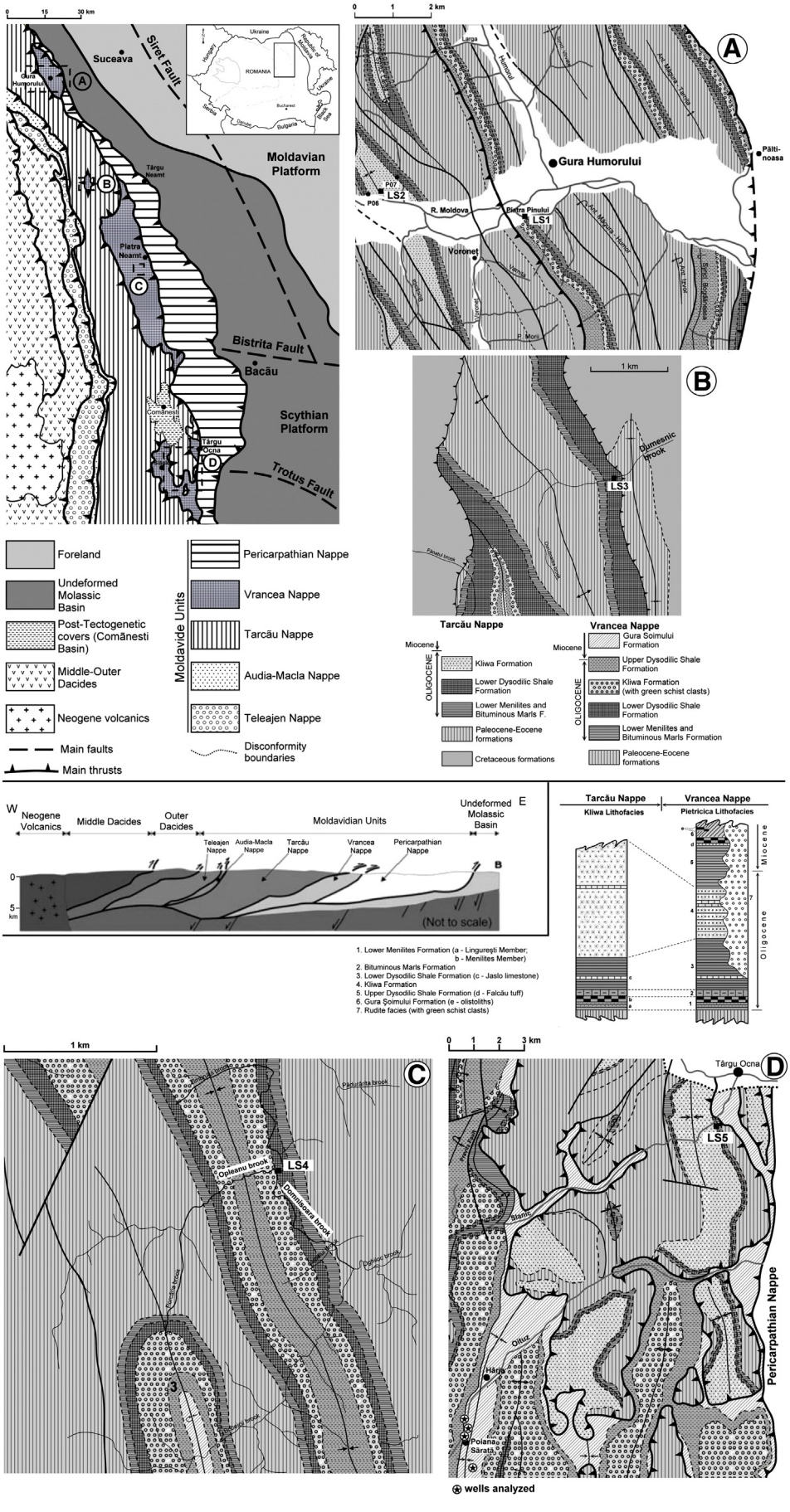
Suceava
Siret Fault
Moldavian Platform
Târgu Neamţ
Piatra Neamţ
Bistrita Fault
Bacău
Comănesti
Târgu Ocna
Scythian Platform
Trotus Fault
Gura Humorului
Gura Humorului
Păltinoasa
R. Moldova
Pietra Pinului
LS1
LS2
P07
P06
Voronet
LS3
Dumesnic brook
Foreland
Undeformed Molassic Basin
Post-Tectogenetic covers (Comănesti Basin)
Middle-Outer Dacides
Neogene volcanics
Main faults
Main thrusts
Moldavide Units
Pericarpathian Nappe
Vrancea Nappe
Tarcău Nappe
Audia-Macla Nappe
Teleajen Nappe
Disconformity boundaries
Tarcău Nappe
Vrancea Nappe
Miocene
OLIGOCENE
Kliwa Formation
Lower Dysodilic Shale Formation
Lower Menilites and Bituminous Marls F.
Paleocene-Eocene formations
Cretaceous formations
Gura Soimului Formation
Upper Dysodilic Shale Formation
Kliwa Formation (with green schist clasts)
Lower Dysodilic Shale Formation
Lower Menilites and Bituminous Marls Formation
Paleocene-Eocene formations
W
Neogene Volcanics
Middle Dacides
Outer Dacides
Moldavidian Units
Undeformed Molassic Basin
E
Teleajen Nappe
Audia-Macla Nappe
Tarcău Nappe
Vrancea Nappe
Pericarpathian Nappe
(Not to scale)
1. Lower Menilites Formation (a - Lingureşti Member; b - Menilites Member)
2. Bituminous Marls Formation
3. Lower Dysodilic Shale Formation (c - Jaslo limestone)
4. Kliwa Formation
5. Upper Dysodilic Shale Formation (d - Falcău tuff)
6. Gura Şoimului Formation (e - olistoliths)
7. Rudite facies (with green schist clasts)
Tarcău Nappe
Kliwa Lithofacies
Vrancea Nappe
Pietricica Lithofacies
Miocene
Oligocene
Ouleanu brook
LS4
Domnişoara brook
Târgu Ocna
LS5
Pericarpathian Nappe
Poiana Sărată
wells analyzed

Previous palynological studies conducted on the Oligo-Miocene Carpathian Flysch have revealed the presence of higher plant species such as *Alnus*, *Betula*, *Corylus*, *Pinaceae* and *Quercus*, ferns and phytoplankton represented by *Cleistosphaeridium pectiniforme* Garlach, 1961, *Deflandrea phosphoritica* Eisenack, 1938, *Thalassiphora delicata* Williams and Downie, 1966, *T. pelagica* (Eisenack 1954) Eisenack and Gocht, 1960, *Wetzeliella rotundata*, Balteş, 1969 (Olaru, 1978). From the Slănic-Oituz Half-window (Upper Dysodilic Shale Formation), Stoicescu (2004) cites species such as *Baculatisporites nanus* (Wolff 1934) Krutzsch, 1959, *Caryapollenites simplex* (Potonié 1931) Potonié, 1960, *Juglans*, *Laevigatosporites gracilis* Wilson and Webster, 1946, *Magnolipollis* sp., *Monocolpopollenites tranquillus* (Potonié 1934) Thomson and Pflug, 1953, *Pinaceae* and *Tilia*. The palaeoclimate conditions inferred from this palynological assemblage, established using the "Coexistence Approach" method, are characterized by a mean annual temperature between 13.3 and 17.2 °C, and a mean annual precipitation between 578 and 1520 mm. The mean temperature of the coldest month varies from 0.9 to 7 °C, and mean temperature of the warmest month ranges between 23.6 and 28.1 °C (Ţabără and Chirilă, 2012).

3. Materials and methods

The present study focuses on thirty-three samples from the following sedimentary deposits (Table 1): the Bituminous Marls Formation (early Oligocene), the Lower Dysodilic Shale Formation (Rupelian / Chattian) and the Upper Dysodilic Shale Formation (Upper Oligocene–early Miocene). Twenty-five samples originate from outcrops (Fig. 1, LS1–LS5), while eight samples were collected from wells located in the Hârja-Poiana Sărată Syncline.

3.1. Palynological and palynofacies analysis

Twenty samples (see Table 1) were processed using standard palynological techniques (e.g., Batten, 1999). Approximately 50 g of sediments was sampled for organic matter analyses. These samples were treated with HCl (37%) to remove carbonates and HF (48%) to remove the silicate minerals. Denser particles were separated from the organic residue using $ZnCl_2$ with a density of 2.0 g/cm^3. The microscopic slides were made using glycerine jelly as a mounting medium.

Palynofacies analysis as described by Tyson (1995) is an important tool in sedimentology for reconstructing depositional environments and estimating hydrocarbon source rock potential, based on the total assemblage of particulate organic matter. The sedimentary organic matter of the Oligo-Miocene Moldavidian Domain includes a continental fraction, with phytoclasts, pollen grains and spores, as well as a marine fraction composed of dinoflagellate cysts and prasinophyte algae (Table 2). The AOM fraction refers to all particulate organic components that appear structureless under light microscopy, and includes phytoplankton and bacterially derived organic matter, higher plant resins and amorphous products of macrophyte tissue diagenesis (Tyson, 1993, 1995).

The relative percentage of these components is based upon counting of at least 300–400 organic particles (>15 μm) per slide, which was performed using a Leica DM1000 microscope with transmitted white and blue light fluorescence, according to Tyson (1995, 2006). Since AOM was dominant in the analyzed samples, the identification of palynomorph taxa that were hidden by it was performed using blue light fluorescence. Marine and continental palynomorphs have different fluorescence color intensities, allowing detailed observation of their morphology.

We assigned the following interpretive parameters based on palynofacies observations (all ratios are expressed in decimal logarithms; Tyson, 1995):

(i) The relative percentage of total phytoclasts, the abundance of which usually indicates the proximity of a fluvio-deltaic source and tends to decrease distally (Tyson, 1995).

(ii) The continental/marine ratio (CONT/MAR) was calculated using all palynofacies constituents in the present study (organic particles having a continental or marine origin are shown in Table 2). It tends to decrease distally and can be used to interpret proximal–distal trends. Similarly, its stratigraphic variations may indicate transgressive–regressive changes (Steffen and Gorin, 1993).

Following the optical microscopy analyses, ten samples were further investigated using SEM. The palynological residues were dehydrated and Au/Pd-coated before imaging. SEM microphotographs were obtained by means of a Zeiss Supra 50 VP equipped with an energy dispersive spectrometer (EDS) that was used for imaging and elemental analysis of framboidal pyrites at the University of Zürich, Switzerland.

Numerous authors (Combaz, 1980; Batten, 1983; Courtinat et al., 2003; Ercegovac and Kostić, 2006; Pacton et al., 2011; Suárez-Ruiz et al., 2012) have proposed classifications of AOM based on their origin (continental or marine). Terrestrial AOM is generally described as having a gelified appearance, usually with no internal structure, while marine AOM derived from phytoplankton degradation is described as having a "fluffy" or "flakey" granular texture. Its color generally varies from yellow-green under oxic sedimentary conditions in coastal areas, to brown under dysoxic/anoxic conditions in pelagic zones (Masran and Pocock, 1981; Valdés et al., 2004; Ercegovac and Kostić, 2006). Recently, Pacton et al. (2011) suggested a new AOM characterization according to its biological origin, separating the two types: (1) granular AOM with patchy fluorescence (depending on its oxidation state) from marine sources, and derived from microbial reworking, and (2) gelified AOM, with a brown color and sometimes containing internal structures, derived from terrestrial organic matter degraded by bacteria, being a secondary microbial product.

Depending on its composition, visual examination of organic matter isolated from the rock enables assignment of a particular kerogen type. Combaz (1980), Selley (1997), Suárez-Ruiz et al. (2012), and Mendonça Filho et al. (2012) have all distinguished the three types of kerogen by means of optical criteria. Their assignments are well correlated with those obtained using a geochemical approach (e.g., van Krevelen diagram; Tissot and Welte, 1984). Kerogen type I is considered to be of algal origin, with a relatively high H/C ratio and a very low O/C ratio; Type II is of marine origin, with a relatively high H/C ratio and a low O/C ratio; and Type III is essentially derived from continental plants with a low initial H/C ratio and a high initial O/C ratio.

3.2. Geochemical analysis

Organic matter abundance in sediments is usually expressed as the percentage of organic carbon on a dry weight basis. The hydrocarbon generation potential of source rocks can be estimated from this value, ranging from poor to excellent for elevated TOC abundances (Peters and Cassa, 1994). A EuroEa 3000 EuroVector elemental analyzer was used to measure % TOC, H, N, S and O. Samples were first crushed to a particle diameter of 0.1 mm, followed by a 4 N HCl treatment for 24 h in order to remove inorganic carbon (Weiss et al., 2000; Ekpo et al., 2013). The remaining material was then washed with distilled water several times so as to remove the acid, and then dried in an oven at 50 °C.

The elemental abundances obtained from the completely isolated kerogen were used to calculate its H/C and O/C atomic ratios, in order to establish the type of kerogen contained in the original rock (van Krevelen diagram; Fig. 5D). Kerogen extraction was performed following the method described in (Durand and Nicaise, 1980; modified by Vandenbroucke, 2003; Vandenbroucke and Largeau, 2007).

All geochemical results are listed in Table 1.

The Rock-Eval analyses were conducted in the laboratory at the Geolog International Company (Italy). Following pyrolysis, the parameters measured included the S_1 and S_2 (mg HC/ g rock) and T_{max} (°C). Based on these parameters, the Hydrogen Index (HI) S_2/TOCx100 was

Table 1
Elemental geochemical analysis for bituminous rocks from the cross sections analyzed.

	Stratigraphic unit	Outcrops and wells location (Fig. 1)	Method of analysis		Sample	TOC %	H %	O %	N %	H/C ratio	O/C ratio	C/N ratio	S_1	S_2	T_{max}	HI	Petroleum potential after TOC content (Peters and Cassa, 1994)
Vrancea Nappe, Pietricica Lithofacies	Bituminous Marls Formation	LS1 Piatra Pinului section	TOC analysis		P01	8.905	1.66										excellent
	Lower Dysodilic Shale Formation				P02	2.032	0.957										very good
					[a]P03	2.911	1.1										very good
	Upper Dysodilic Shale Formation				[a]P04	1.963	0.889										good
	Bituminous Marls Formation		analysis on kerogen extracted from rock		P01	47.697	5.422	15.79	8.29	1.36	0.248	6.712					
	Lower Dysodilic Shale Formation				P02	52.012	5.245	15.59	14.965	1.21	0.224	4.058					
	Upper Dysodilic Shale Formation				P05	44.07	5.48	18.14	7.02	1.492	0.308	7.329					
Tarcău Nappe, Kliwa Lithofacies	Lower Dysodilic Shale Formation	LS2 Frasin section	TOC analysis		[a]P06	1.652	1.043										good
					[a]P07	4.316	1.32										excellent
Vrancea Nappe, Pietricica Lithofacies	Lower Dysodilic Shale Formation	LS4 Domnişoara section	TOC analysis		[a]P08	2.503	1.018										very good
					[a]P09	4.49	1.105										excellent
					[a]P10	2.472	0.958										very good
Tarcău Nappe, Kliwa Lithofacies	Lower Dysodilic Shale Formation	LS5 Slănic section	TOC analysis		P11	7.729	1.393										excellent
					[a]P12	2.14	1.03						0.09	4.9	419	228.9	very good
					P13	2.18	0.744										very good
					[a]P14	5.435	1.368										excellent
					P15	2.186	0.997										very good
					[a]P16	3.21	1.092						0.19	8.48	427	264.1	very good
					P17	17.59	2.49										excellent
					[a]P18	3.791	1.23										very good
					P19	2.786	1.107										very good
					[a]P20	2.41	1.132						0.28	6.3	429	261.4	very good
					P21	2.409	1.069										very good
					[a]P22	2.582	1.008										very good
Vrancea Nappe, Pietricica Lithofacies	Upper Dysodilic Shale Formation	Samples analyzed from wells (Hârja – Poiana Sărată syncline)	TOC analysis	SX6	[a]P23 (1049 m)	1.874	0.481										good
					P24 (1057 m)	3.259	1.328										very good
					P25 (1076 m)	9.966	1.379										excellent
				SX7	P26 (909 m)	6.044	1.258										excellent
					[a]P27 (920 m)	2.348	0.645										very good
				SX2	P28 (930 m)	3.074	1.15										very good
					[a]P29 (941 m)	2.942	1.231										very good
				SY5	[a]P30 (724 m)	2.905	0.66										very good

[a] Samples used for palynological and palynofacies analyzes.

Table 2
Classification of sedimentary organic matter (modified after Tyson, 1995; Bombardiere and Gorin, 2000; Mendonça Filho et al., 2002; Carvalho et al., 2006; Ercegovac and Kostić, 2006).

Group	Subgroup		Origin	
Phytoclasts	Opaque	Equidimensional	Derived from the ligno-cellulosic tissues of terrestrial higher plants or fungi.	Continental
		Lath		
	Translucent	Cuticle	Leaf-epidermal tissue of higher plants	
		Membranes	Thin, non-cellular, transparent sheets of probable plant origin.	
		Woody tissues (secondary xylem)	Gymnosperm and Angiosperm tracheid tissue	
		Fungal hyphae	Derived from fungi	
Palynomorphs	Sporomorph	Spores	Terrestrial palynomorph produced by Pteridophyte, Briophyte and fungi.	
		Pollen grains	Terrestrial palynomorph produced by Gymnosperm and Angiosperm plants.	
	Phytoplankton	Chlorococcale algae	Exclusively colonial freshwater algae (*Botryococcus* and *Pediastrum*).	
		Dinoflagellate cysts	Resting cysts produced during the sexual part of the life cycle of Class Dinophyceae survives.	Marine
		Prasinophytes	Fossilizing structures produced by small quadriflagellate algae (Division Pyrrhophyta). Most, like *Tasmanites*, are spherical; diameter 50–2000 μm, smooth and thick-walled.	
		Acritarchs	Small microfossils of unknown and probably varied biological affinities.	
	Zoomorph	Foraminiferal test linings	Organic linings of benthic foraminifera.	
		Scolecodonts	Mouth parts of some polychaete worms (mostly marine).	
Amorphous organic matter	AOM		Derived from phytoplankton or degradation of bacteria (fluorescent AOM) or degraded higher plant debris (non-fluorescent AOM). Structureless material with no morphology or form. Color: yellow-orange-red; orange-brown; gray. Heterogeneity: homogeneous; with "speckles"; clotted; with inclusions (palynomorphs, phytoclasts, pyrite). Form: flat; irregular; angular; pelletal (rounded eleongate/oval shape). AOM usually dominates sediments deposited in oxygen deficient conditions.	Continental
	Resin		Derived from higher plants of tropical and subtropical forest. Structureless particle, hyaline, homogeneous, non-fluorescent, rounded, sharp to diffuse outline.	

calculated and plotted on a van Krevelen diagram (HI versus T_{max}; Fig. 5A). The Rock-Eval pyrolysis analyses consisted of three samples collected from the LS5 geological section.

3.3. Thermal maturity

Organic matter thermal maturity was determined using the Thermal Alteration Index (TAI; Staplin, 1969; Pearson, 1984), the fluorescence color and T_{max}.

The TAI is a scale (with values from 1 to 5) used to estimate the thermal maturation of organic matter, and is based on palynomorph color observed using a transmitted light microscope. With an increase in thermal maturity, the color of the palynomorphs changes from yellow (TAI = 1–2 for the immature phase, corresponding to a vitrinite reflectance VRo of up to 0.5%), to dark yellow-orange (TAI = 2+ − 3+ for the mature phase, where VRo is between 0.5 and 1.3%), to dark-brown or black (TAI = 3+ to 4–5, corresponding to an over-mature stage) (Pearson, 1984; Smojić et al., 2009). This gradual change in color is due to an increase in the depth and temperature at which spores and pollen are buried, causing chemical changes in the composition of palynomorph exine.

Fluorescence microscopy is another important method used in the assessment of thermal maturity and hydrocarbon generation potential, and is based on the fluorescence intensity and color of the organic matter (e.g., van Gijzel, 1967; Raynaud and Robert, 1976; Robert, 1985; Tyson, 2006; Smojić et al., 2009; Suárez-Ruiz et al., 2012). Here we use the fluorescence rank of prasinophyceans (Robert, 1985). Over the course of maturation, prasinophyceans exhibit high fluorescence intensity in green to golden-yellow colors up to vitrinite reflectance (VRo) ~ 0.7%, orange colors with decreasing fluorescence intensity at VRo ~ 0.7–0.9%, and red colors with low fluorescence intensity at VRo ~ 0.9%–1.2% (Smojić et al., 2009). A type I3 (BP 450–490) fluorescence filter was used in order to view organic matter in blue light.

T_{max} was also used to estimate the thermal evolution of the organic matter. Values increase with maturity. T_{max} values < 430 °C suggest immature organic matter, values between 430 and 465 °C represent the oil window (mature organic matter), and T_{max} > 465 °C defines the over-mature zone.

4. Results and interpretation

4.1. Palynological assemblages

The Lower Dysodilic Shale Formation (Tarcău and Vrancea Nappes) exhibits an abundance and diversity of dinoflagellate cysts and prasinophyte algae, in association with *Pinaceae* pollen. A taxonomic diversification of continental palynomorphs becomes noticeable with the onset of Upper Dysodilic Shale Formation sedimentation, and out of the phytoplankton species, only *Tytthodiscus* sp. and *Deflandrea phosphoritica* persist. The taxonomic list of palynomorphs and their relative occurrence in the analyzed deposits is presented in Appendix 1.

4.1.1. Lower Dysodilic Shale Formation, LS5 (Slănic section, Tarcău Nappe)

Although TOC values remain high overall, with substantial variations (values ranging from 2 to 6%), these samples are dominated by AOM (more than 95%) (Fig. 2). Both the lower and upper parts of this unit likely represent marine conditions, as suggested by the CONT/MAR ratio. Slight continental influences characterize the middle section, indicating a more proximal environment, as shown, again, by the CONT/MAR ratio. Phytoplankton (dinoflagellate cysts and prasinophytes) represent 74% of all palynomorphs, while pollen and spores account for 26%. *Tytthodiscus* is the most abundant marine palynomorph species (28%). Other species were found as well, such as *Deflandrea phosphoritica*, *Homotryblium plectilum*, *Hystrichokolpoma rigaudiae*, *Rhombodinium draco*, *Thalassiphora pelagica*, and reworked species such as *Rhombodinium perforatum* (dating from Eocene). Continental palynomorphs are dominated by *Pinaceae* pollen, whereas palm trees pollen (*Monocolpopollenites tranquillus*), *Corylus*, *Cyrilla*, *Ulmus* and ferns constitute a minor fraction.

4.1.2. Lower Dysodilic Shale Formation, LS4 (Domnişoara section, Vrancea Nappe)

The palynofacies data obtained for the lower part of the Domnişoara section are similar to those from the Slănic section in terms of palynofacies distribution, TOC and CONT/MAR ratio. Sample P09 exhibits a decreasing continental influence (the absence of translucent phytoclasts) in this distal setting, with higher TOC values (up to 5%). The AOM content exceeds 95%. Palynomorphs are dominated by dinoflagellates such as *Deflandrea*

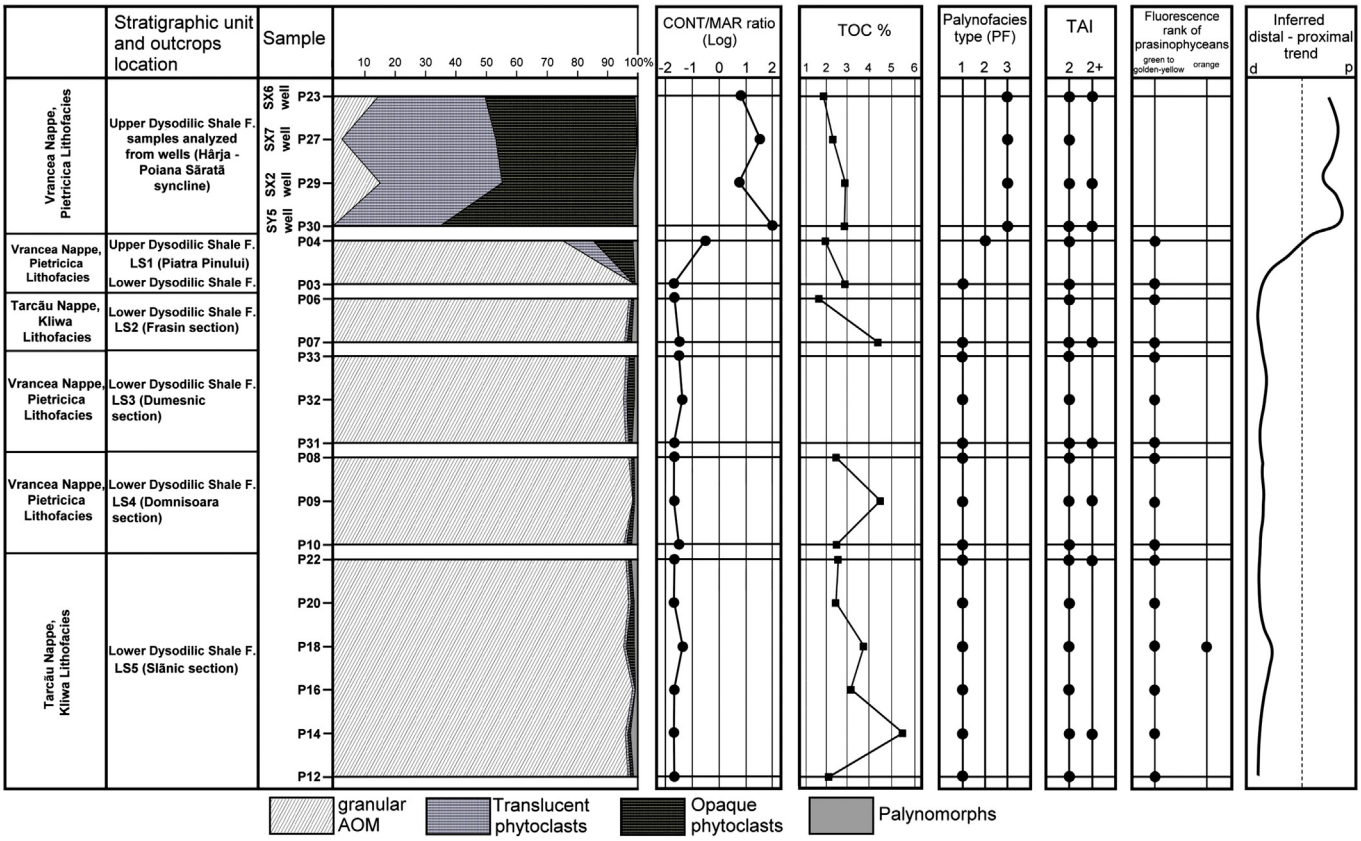

Fig. 2. Relative abundance of selected kerogen groups from the analyzed samples (percentage calculated to Total Sedimentary Organic Matter). The diagram shows TAI values, fluorescence rank, the CONT/MAR ratio and TOC content for each sample analyzed.

phosphoritica, *Enneadocysta* aff. *pectiniformis*, *Homotryblium plectilum*, *Hystrichokolpoma rigaudiae*, *Lingulodinium machaerophorum* and *Thalassiphora pelagica*. Gymnosperms (*Pinaceae* and *Taxodiaceae*) are the sole continental palynomorphs occurring in the palynological assemblage, with a 7% abundance.

4.1.3. Lower Dysodilic Shale Formation, LS3 (Dumesnic section, Vrancea Nappe)

The palynofacies assemblage is dominated by AOM, which accounts for more than 95% of the sample. The low CONT/MAR ratio suggests a more distal setting (Fig. 2). Among the palynomorphs, the most abundant type of dinoflagellate is *Homotryblium* (*H. plectilum*, *H. aculeatum*, *H. vallum*), while *Cordosphaeridium inodes*, *Deflandrea phosphoritica*, *Operculodinium centrocarpum*, *Polysphaeridium subtile* and *Thalassiphora pelagica*, are of minor importance. Only gymnosperm pollen is present, such as *Pinaceae* and *Taxodiaceae* (5%).

4.1.4. Lower Dysodilic Shale Formation, LS2 (Frasin section, Tarcău Nappe)

The organic matter from the Frasin section exhibits a slight increase in palynomorph abundance, compared to the samples described above, but is still dominated by AOM (>95%). The setting was more distal, as suggested by the CONT/MAR ratio, and a decrease in TOC abundance was observed, from 4 to 2%. The palynomorphs are dominated by dinoflagellates, such as *Cordosphaeridium gracile*, *Deflandrea phosphoritica*, *Homotryblium plectilum*, *Palaeocystodinium golzowense*, *Spiniferites* sp., *Thalassiphora pelagica* and *Wetzeliella gochtii*. Continental palynomorphs chiefly consist of *Pinaceae* and *Taxodiaceae*.

4.1.5. Lower Dysodilic Shale and Upper Dysodilic Shale Formations, LS1 (Piatra Pinului section, Vrancea Nappe)

From the lower part of Piatra Pinului section, sample P03 (assigned to the Lower Dysodilic Shale Formation) exhibits the most abundant AOM (>97%), while sample P04 (collected from the Upper Dysodilic Shale Formation) reveals a significant increase in opaque and translucent phytoclasts (up to 30% of the total assemblage). These parameters, as well as the CONT/MAR ratio, suggest a more proximal marine environment.

This section was previously described by Ţabără (2010). Palynomorphs consist of a limited number of species, such as *Dracodinium* sp. (reworked from Eocene), *Pityosporites* sp., *Sciadopityspollenites* sp. and *Spiniferites ramosus*. Prasinophyte algae (*Tytthodiscus* sp.) represent the sole palynomorphs identified in sample P04.

4.1.6. Upper Dysodilic Shale Formation (Hârja – Poiana Sărată syncline, Vrancea Nappe)

The samples drilled from the Hârja – Poiana Sărată syncline are marked by a drastic change, compared to the sections described above. For example, the AOM content varies between less than 1% and 15% and phytoclasts are dominant in the assemblage (83–97%), clearly indicating proximal conditions (Fig. 2). However, the abundance of palynomorphs in these samples is within the same range as that of the other sections. Marine palynomorphs are represented by *Deflandrea phosphoritica* and *Tytthodiscus* sp., while the continental palynomorphs are predominantly *Engelhardia*, *Myrica*, *Quercus*, *Pityosporites*, *Sapotaceae*, *Taxodium* and ferns.

4.1.7. Palaeoecological significance of dinoflagellates

Dinocysts are highly sensitive indicators for changes in (i) surface water productivity, temperature and salinity, (ii) changes in distance from the shore and (iii) stratification and ventilation of the water column in a wide variety of marine settings (Sluijs et al., 2005). The very low proportion of dinocyst-dominated palynomorphs in the studied samples suggests dysoxic, deep-water conditions (Wood and Gorin, 1998). However, certain species can be useful for determining the

paleoecological conditions present during deposition of the Lower and Upper Dysodilic Shale Formations, as follows.

Water salinity is interpreted from taxa of *Homotryblium* div. sp. and *Operculodinium centrocarpum*. According to Köthe (1990), the abundance of *Homotryblium* (mainly *H. plectilum*) suggests a normal salinity. In the Lower Dysodilic Shale Formation (LS1–LS5), this genus is present in both in the Tarcău and Vrancea Nappes, but to a greater extent during deposition of the Dumesnic section (LS3). The other taxon, *Operculodinium centrocarpum*, does not show any variation in the Lower Dysodilic Shale Formation and displays an increased process length. According to de Vernal et al. (1989), there is a relationship between process length and salinity (the length of the process decreases with the decrease in salinity). The specimens we identified have a greater process length, thus suggesting normal salinity.

Water temperature can be established based on *Homotryblium* and *Spiniferites ramosus*. The "*Homotryblium* Complex" appears to reflect warm temperate to tropical palaeo-oceanographic provinces (de Verteuil and Norris, 1996) and *Spiniferites ramosus* is generally considered a warm surface water species (Wall et al., 1977; Harland, 1983; Marret and Zonneveld, 2003).

The oxygen content in the water column can be inferred from specific taxa, such as species of *Thalassiphora pelagica*, which indicate a low-oxygen shelf environment (Köthe, 1990; Pross and Schmiedl, 2002). These species were only identified in the Lower Dysodilic Shale Formation (Tarcău and Vrancea Nappes), without changes in abundance. Changes in dinoflagellate assemblage as a response to oxygen depletion at the water–sediment interface and in the water column of an epicontinental setting have also been observed in early Oligocene sediments (Pross, 2001).

The nutrient content (e.g., phosphate and nitrate) of seawater can be estimated based on some dinoflagellate species that inhabited the photic zone of marginal marine settings. In general, the *Deflandrea*-group, *Rhombodinium* and *Wetzeliella*, present in the Lower Dysodilic Shale Formation, indicate an increased nutrient content, but in well-mixed rather than stratified (coastal) waters (Pross and Schmiedl, 2002; Sluijs et al., 2005; Iakovleva, 2011). *Thalassiphora pelagica* and *Lingulodinium machaerophorum* also suggest growth in nutrient-rich water masses. Some species of dinoflagellates found in the Lower Dysodilic Shale Formation are still living in present-day marine settings. According to Zonneveld et al. (2013), phosphate and nitrate would have ranged between 0.22 and 1.1 μmol/l and 0.6 to 12 μmol/l respectively based on the nutrient tolerance of *Lingulodinium machaerophorum*, *Operculodinium centrocarpum* and *Spiniferites ramosus*.

4.2. Age assignment

The dinocyst assemblages from all sections studied contain few taxa known to represent biostratigraphic markers for the Oligocene. A dinoflagellate cyst zonal scheme has not yet been established for the Paleogene deposits of the Eastern Carpathians. The biostratigraphic interpretation in the present study is therefore based on dinocyst zonations established in Italy (Pross et al., 2010), Germany (Köthe, 1990, 2003, 2005; Köthe and Piesker, 2007), the southeastern part of the North Sea basin (Dybkjær and Piasecki, 2010), Belgium (Van Simaeys et al., 2005) and the Polish Carpathians (Gedl, 2005; Barski and Bojanowski, 2010).

The following marker taxa were identified and used to interpret biostratigraphic successions (Fig. 3):

- *Wetzeliella gochtii* was identified in the Lower Dysodilic Shale Formation (Frasin section) and is considered by most authors as a marker for the early Oligocene. Pross et al. (2010) assigned this taxon to the early Oligocene, between 33.1 and 26.4 Ma (early Rupelian–middle Chattian). In Germany, Köthe and Piesker (2007) assigned *W. gochtii* to the D13–D14 biozones, the last occurrence of this species being synchronous with the Rupelian–Chattian boundary. For the northern part of Europe, Van Simaeys et al. (2005) described it in the Rupelian–middle Chattian, while in southern Poland (Krosno Formation) it was found in the Rupelian (Barski and Bojanowski, 2010).
- *Rhombodinium draco* (Plate II, 2a, 2b, 10) specimens were also found in the Lower Dysodilic Shale Formation (Slănic section). Recently, this taxon has often been associated with the upper Eocene–early Oligocene interval. Therefore, Köthe and Piesker (2007) assigned this taxon to the D11–D14 biozones, which last occurred at the Rupelian–Chattian boundary. Van Simaeys et al. (2004, 2005) determined the same stratigraphic distribution of this species for northern Europe (Belgium). *R. draco* has also been found in Rupelian

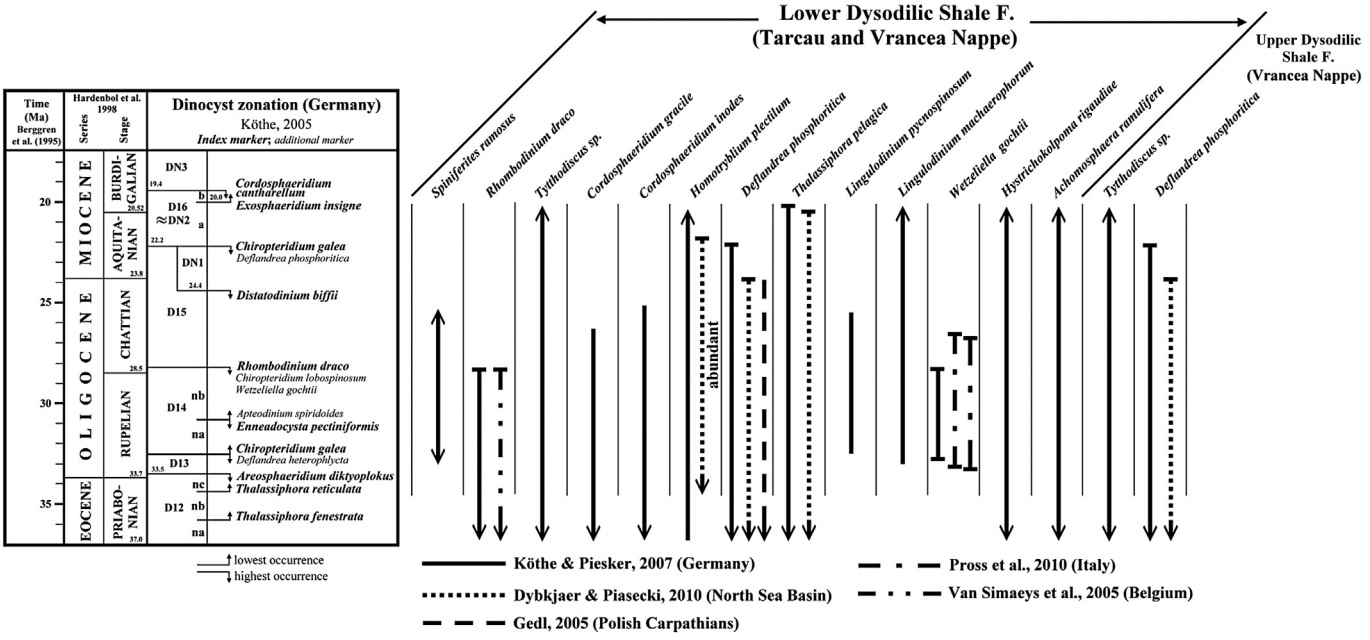

Fig. 3. Range chart of the dinoflagellate cysts used in this study. Correlation with previously published dinocyst zonations within Germany (Köthe and Piesker, 2007), the North Sea Basin (Dybkjær and Piasecki, 2010), Polish Carpathians (Gedl, 2005), Italy (Pross et al., 2010), and Belgium (Van Simaeys et al., 2005) are shown.

deposits of the Krosno Formation from southern Poland (Barski and Bojanowski, 2010) and in the Magura Formation (Gedl, 2005).

– *Cordosphaeridium gracile* and *C. inodes* were identified in the Lower Dysodilic Shale Formation (Frasin section). According to Köthe and Piesker (2007), the last occurrence of these taxa is Chattian (D15 biozone), from the Oligocene deposits of Germany. Both species were noted in the southern part of the Russian Platform in the early Oligocene (Zaporozhets, 1998).

The biostratigraphic information provided by these index species, identified here in the Lower Dysodilic Shale Formation, suggest a Rupelian–early Chattian age (dinocyst zone D14–lower part of D15; Köthe and Piesker, 2007). We note that all index taxa were identified only in the Tarcău Nappe.

The age of the Upper Dysodilic Shale Formation is more difficult to establish due to low dinoflagellate cyst abundances. However, the presence of *Deflandrea phosphoritica* up to the upper part of the formation indicates that it is older than the middle Aquitanian. The last occurrence of *D. phosphoritica* was found above the DN1 zone (middle Aquitanian) in Germany (Köthe and Piesker, 2007) and the Chattian–Aquitanian boundary in the southeastern North Sea Basin (Dybkjær and Piasecki, 2010).

4.3. Palynofacies types

The microscopic study of organic matter allowed determination of three types of palynofacies (PF-1 to PF-3) (Fig. 2). These were established according to the distribution of the three major groups of organic matter: AOM, palynomorphs and phytoclasts (opaque and translucent).

4.3.1. Palynofacies-type 1 (PF-1)

PF-1 is characteristic of all samples collected from the Lower Dysodilic Shale Formation (Tarcău and Vrancea Nappes) (Fig. 2). It is characterized by a large proportion of AOM (95–98%), woody tissues (1–2%), opaque phytoclasts (1–3%) and palynomorphs (1–2%).

The AOM identified in PF-1 has a granular texture and a color ranging from yellow to brown (see Plate III, 1, 2). The granular AOM and fragments of woody tissues sometimes contained framboidal pyrite (Plate IV, 2, 3). Woody tissues (1–2%) (Plate IV, 7) were typically dark brown to black, and the equidimensional opaque phytoclasts (1–3%) belong to the inertinite group (Ercegovac and Kostić, 2006; Charles, 2009; Pacton et al., 2011). These allochthonous phytoclasts have no visible internal structure and sizes of 60–70 μm, often displaying an angular shape. Palynomorphs (1–2%) are mainly composed of dinoflagellate cysts and prasinophyte algae. Terrestrial palynomorphs (spores and pollen) are rare, and are predominantly *Pinaceae* pollen. AOM fluorescence is either weak or absent (Plate IV, 4), perhaps due to bacterial degradation under dysoxic or anoxic conditions, which can lead to decreased fluorescence. Gelified AOM of terrestrial origin sometimes occurs in association with granular AOM (Plate III, 1).

SEM investigations of PF-1 revealed an abundance of bacteria, either as single entities (Plate V, 1, 3) or in colonies (Plate V, 6), and associated EPS (Plate VI, 1–3), which were found covering algal tissues (Plate V, 2). Dinoflagellates are well preserved as shown by intact surfaces and processes (Plate V, 5). Some framboidal pyrites were recognized in the SEM pictures (Plate VI, 4). This facies was deposited in a distal suboxic–anoxic basin (Fig. 4) and is characterized by type II oil prone kerogen (Tyson, 1995).

4.3.2. Palynofacies-type 2 (PF-2)

PF-2 is represented only in one sample collected from the bottom of the Upper Dysodilic Shale Formation (P04, Piatra Pinului section, LS1). The AOM exhibits a lower proportional abundance compared to PF-1 (~75%), with a granular texture and light brown color (Plate III, 2). PF-2 contains small fragments of brown woody tissue (10%) and echidimensional opaque phytoclasts (~13%, inertinite group) with angular or rounded shapes. Palynomorphs (~2%) consist of prasinophyte algae with different fluorescence intensities (bright yellow/pale) (Ţabără, 2010). As in PF-1, the AOM contains coccoid bodies (bacteria or algae), algal filaments and EPS. Terrestrial organic fragments are undergoing microbial degradation, as demonstrated by EPS-covered surfaces (Plate VI, 5). The sticky EPS network allowed preservation of prokaryote cellular division (Plate VI, 6). AOM particles exhibit weak fluorescence. This facies may suggest a dominance of type II (oil-prone) kerogen.

4.3.3. Palynofacies-type 3 (PF-3)

PF-3 is characteristic of the middle and upper parts of the Upper Dysodilic Shale Formation. It was identified in samples collected from 4 wells located in the Slănic-Oituz Half-window (Hârja – Poiana Sărată syncline, Vrancea Nappe).

The phytoclast group is highly abundant (83–98%) in this type of palynofacies (Plate III, 3). Opaque fragments are generally equidimensional, rounded or angular, and associated with brown woody tissues and cuticles. The palynomorph group (1–2%) is dominated by gymnosperm and angiosperm pollen, and by phytoplankton (*Deflandrea* and *Tytthodiscus*). The AOM (1–15%) in PF-3 contains both granular and gelified types (Plate IV, 8), indicating marine and terrestrial origins, respectively. It is non-fluorescent or displays weak fluorescence. Filamentous and coccoid bacterial colonies can be observed colonizing terrestrial fragments (Plate VII, 2, 3), and abundant framboidal pyrites are also present (Plate VII, 1, 4, 5). According to Tyson (1995); (Fig. 4), this facies is dominated by type III (gas-prone) kerogen.

4.4. Palaeoenvironmental reconstruction of the Oligo-Miocene formations from the Moldavidian Domain

4.4.1. Distal suboxic-anoxic basin

The Lower Dysodilic Shale Formation is characterized by PF-1 and exhibits the highest AOM content (more than 90%), includes *Thalassiphora pelagica*, which suggests suboxic–anoxic environmental conditions throughout the palaeo-water column (Köthe, 1990; Tyson, 1995; Pross and Schmiedl, 2002). Such a dominant kerogen constituent is characteristic of distal dysoxic to anoxic shelf environments (Tyson, 1995). According to organic matter classifications (see references above), the AOM is dominantly granular and of marine origin. A yellow color suggests accumulation in suboxic environments (Plate IV, 1), and possibly anoxic conditions when the AOM color is dark brown (Plate III, 1). The SEM investigations performed on this AOM suggest that it is mainly of microbial origin, as shown by the numerous bacteria and associated EPS, which are related to high primary productivity. A marine origin for the AOM is supported by the C_{org}/N ratio (Meyers, 1994; Fig. 5C). Dinoflagellate distributions indicate warm temperate growth waters, while *Homotryblium* div. sp. and *Operculodinium centrocarpum* suggest normal salinity conditions (Islam, 1984; Köthe, 1990). Nutrient rich waters can be deduced from *Deflandrea*, *Lingulodinium machaerophorum*, *Rhombodinium* and *Wetzeliella* taxa.

These data are in agreement with the hypothesis that the deposition of black shales from the Lower Dysodilic Shale Formation occurred in a deep basin, periodically isolated, where basin evolution was controlled by compressional tectonic activity affecting the system margin (Belayouni et al., 2009). The dominance of AOM associated with no increase in quartz content, as well as the absence of changes in sedimentary fabrics, confirm depositions in a distal, reducing environment which was not affected by gravity flows or bottom currents.

4.4.2. Marginal dysoxic–anoxic basin

A decrease in AOM content, coupled with an increase in phytoclasts, indicates a regression and/or an increase in terrestrial influx in

the lower part of the Upper Dysodilic Shale Formation, which is characterized by PF-2. The AOM displays the same features as in PF-1, suggesting a marine microbial origin. Phytoclasts (~25%) consist of small woody tissues and inertinite fragments with angular or rounded shapes. The decrease in dinoflagellate diversity might be explained by the dilution of marine microfossils due to high sedimentation rate or low cyst fluxes related to low productivity (Candel et al., 2012).

4.4.3. Highly proximal shelf or basin

The Upper Dysodilic Shale Formation, defined by PF-3, exhibits a clear proximal signature, as demonstrated by the dominance of phytoclasts (83–98%) and a taxonomic diversification of continental palynomorphs. It also has a significantly lower AOM content (less than 15%). The proximal sections (Upper Dysodilic Shale Formation) are characterized by a high amount of prasinophytes in the plankton group, while dinoflagellate cysts dominate the distal sections (Lower Dysodilic Shale Formation) (Götz et al., 2008). The AOM is both granular and gelified, confirming a microbial origin and degradation of terrestrial fragments. Anoxic conditions persisted at the water–sediment interface, as shown by the presence of framboidal pyrite. Waters were nutrient-rich during the entire deposition of the Upper Dysodilic Shale Formation as shown by the continuous presence of the *Deflandrea* genus.

4.5. Hydrocarbon source potential

Across the Slănic section (LS5; Tarcău Nappe), the Lower Dysodilic Shale Formation has an oil and gas potential that is between very good and excellent, sometimes with high values of TOC (up to 17%). The kerogen maturity given by TAI values is between 2 and 2+ (the limit between immature and mature), while the prasinophyte algae fluorescence frequently ranges from golden yellow to green (VRo up to 0.7%; Plate I, 3a) and, rarely, to orange (VRo ~ 0.7–0.9%; Plate I, 2a).

Plate I. (scale bar: 25 μm)

1. (incident blue light, fluorescence): a — *Cordosphaeridium gracile* (Eisenack 1954) Davey and Williams, 1966; b — *Cordosphaeridium inodes* (Klumpp 1953) Eisenack, 1963 (P07 sample, LS2 section).
2a. (incident blue light, fluorescence), 2b (Idem, transmitted light): *Tytthodiscus* sp. (P18 sample, LS5 section). In blue light this taxon shows an orange color (VRo ~ 0.7-0.9%).
3a. (incident blue light, fluorescence), 3b (Idem, transmitted light): *Tytthodiscus* sp. (P14 sample, LS5 section). In blue light this taxon shows a green to golden-yellow color (VRo up to 0.7%).
4. (incident blue light, fluorescence): *Homotryblium vallum* Stover, 1977 (P32 sample, LS3 section).
5a. (incident blue light, fluorescence), 5b (Idem, transmitted light): *Homotryblium plectilum* Drugg et Loeblich Jr 1967 (P10 sample, LS4 section).
6. (incident blue light, fluorescence): *Operculodinium centrocarpum* (Deflandre and Cookson, 1955) Wall, 1967 (P06 sample, LS2 section).
7. (incident blue light, fluorescence): *Wetzeliella gochtii* Costa and Downie, 1976 (P06 sample, LS2 section).
8a. (incident blue light, fluorescence), 8b (Idem, transmitted light): *Thalassiphora pelagica* (Eisenack, 1954) Eisenack and Gocht, 1960 (P22 sample, LS5 section).

Plate II. (scale bar: 25 μm). (see on page 12)

1. (transmitted light): *Palaeocystodinium golzowense* Alberti, 1961 (P03 sample, LS1 section).
2a. (incident blue light, fluorescence), 2b(Idem, transmitted light): *Rhombodinium draco* Gocht, 1955 (P22 sample, LS5 section).
3. (transmitted light): *Polypodiaceoisporites* sp. (P23 sample, SX6 well). TAI = 2+ (mature phase for hydrocarbon generation).
4. (transmitted light): *Pityosporites labdacus* (Potonie 1931) Thomson and Pflug, 1953 (P12 sample, LS5 section). TAI = 2 (immature phase for hydrocarbon generation).
5. (incident blue light, fluorescence): *Hystrichokolpoma rigaudiae* Deflandre and Cookson, 1955 (P22 sample, LS5 section).
6. (incident blue light, fluorescence): *Polysphaeridium subtile* Davey and Williams, 1966 (P31 sample, LS3 section).
7a. (incident blue light, fluorescence), 7b (Idem, transmitted light): *Deflandrea phosphoritica* Eisenack, 1938 (P22 sample, LS5 section).
8. (incident blue light, fluorescence): *Spiniferites ramosus* (Ehrenberg 1838) Mantell 1854 (P32 sample, LS3 section).
9. (transmitted light): *Monocolpopollenites tranquillus* (Potonié 1934) Thomson and Pflug, 1953 (P12 sample, LS5 section). TAI = 2- (immature phase for hydrocarbon generation).
10. (incident blue light, fluorescence): *Rhombodinium draco* Gocht, 1955 (P22 sample, LS5 section).
11. (transmitted light): *Sapotaceoidaepollenites* sp. (P30 sample, SY5 well). TAI = 2+ (mature phase for hydrocarbon generation).
12. (transmitted light): *Cyrillaceaepollenites exactus* (Potonié 1931) Potonié, 1960 (P22 sample, LS5 section). TAI = 2- (immature phase for hydrocarbon generation).

Plate III. (scale bar: 100 μm). Representative palynofacies assemblages from the Oligocene of the Eastern Carpathians (all unoxidized residues). (see on page 13)

A. PF-1 (Lower Dysodilic Shale Formation, P14, Slănic section, Tarcău Nappe). Abundant AOM (granular and gelified) with dark brown color in association with algal filaments and phytoclasts. The color and abundance of AOM suggest a dysoxic–anoxic environment. The sample containing this organic matter has a TOC content of 5.4% and it can be assigned as kerogen type II (oil prone). Granular AOM (black arrow), gelified AOM (blue arrow), algal filament (red arrow).
B. PF-2 (Upper Dysodilic Shale Formation, P04, Piatra Pinului section, Vrancea Nappe). Granular AOM with a yellow to light-brown color (OMG) in association with black or brown phytoclasts (PHY) and palynomorphs (PAL). The depositional environment was mainly dysoxic, and the sample has a TOC content of 1.96%.
C. PF-3 (Upper Dysodilic Shale Formation, P30, SY5 well, Vrancea Nappe). Abundant organic matter in black and brown phytoclasts (PHY), rounded and angular, suggests a marginal dysoxic basin. The kerogen can be type III (gas prone). This sample has TOC = 2.9%.

Plate IV. (scale bar: 50 μm). In a palynological slide under natural light and blue-light fluorescence, examples of the constituents of the different palynoclast groups used in this study. (see on page 13)

1. Yellow granular AOM with a diffuse edge, in association with coccoid bodies (bacteria or algae, black arrow). The AOM color indicates an oxic-dysoxic depositional environment. (Lower Dysodilic Shale Formation, P33, Dumesnic section, Vrancea Nappe).
2. Brown woody tissue with framboidal pyrite (Lower Dysodilic Shale Formation, P20, Slănic section, Tarcău Nappe).
3. Under natural light, granular brown AOM containing framboidal pyrite. The depositional environment was dysoxic–anoxic with well-preserved organic matter. This organic matter represents a type II kerogen (HI = 261.4 mg HC/g TOC and T_{max} = 429 °C) at the limit between the immature and mature stages of hydrocarbon generation (Lower Dysodilic Shale Formation, P20, Slănic section, Tarcău Nappe).
4. Idem previous image (blue-light fluorescence). This AOM does not show fluorescence due to bacterial degradation.
5. Under natural light, brown AOM in association with coccoid bodies (black arrow), filamentous bacteria (white arrow), EPS (blue arrow, tiny filaments forming an alveolar network) and pollen (red arrow) (Lower Dysodilic Shale Formation, P22, Slănic section, Tarcău Nappe).
6. Idem previous image (blue-light fluorescence). AOM exhibits weak fluorescence.
7. Under natural light, black woody tissue (terrigenous phytoclast) showing fibrous parallel structure in association with granular AOM (Lower Dysodilic Shale Formation, P14, Slănic section, Tarcău Nappe).
8. Under natural light, dark brown gelified AOM (terrestrial fragment) found in an advanced stage of degradation (Upper Dysodilic Shale Formation, P29, SX2 well, Vrancea Nappe).

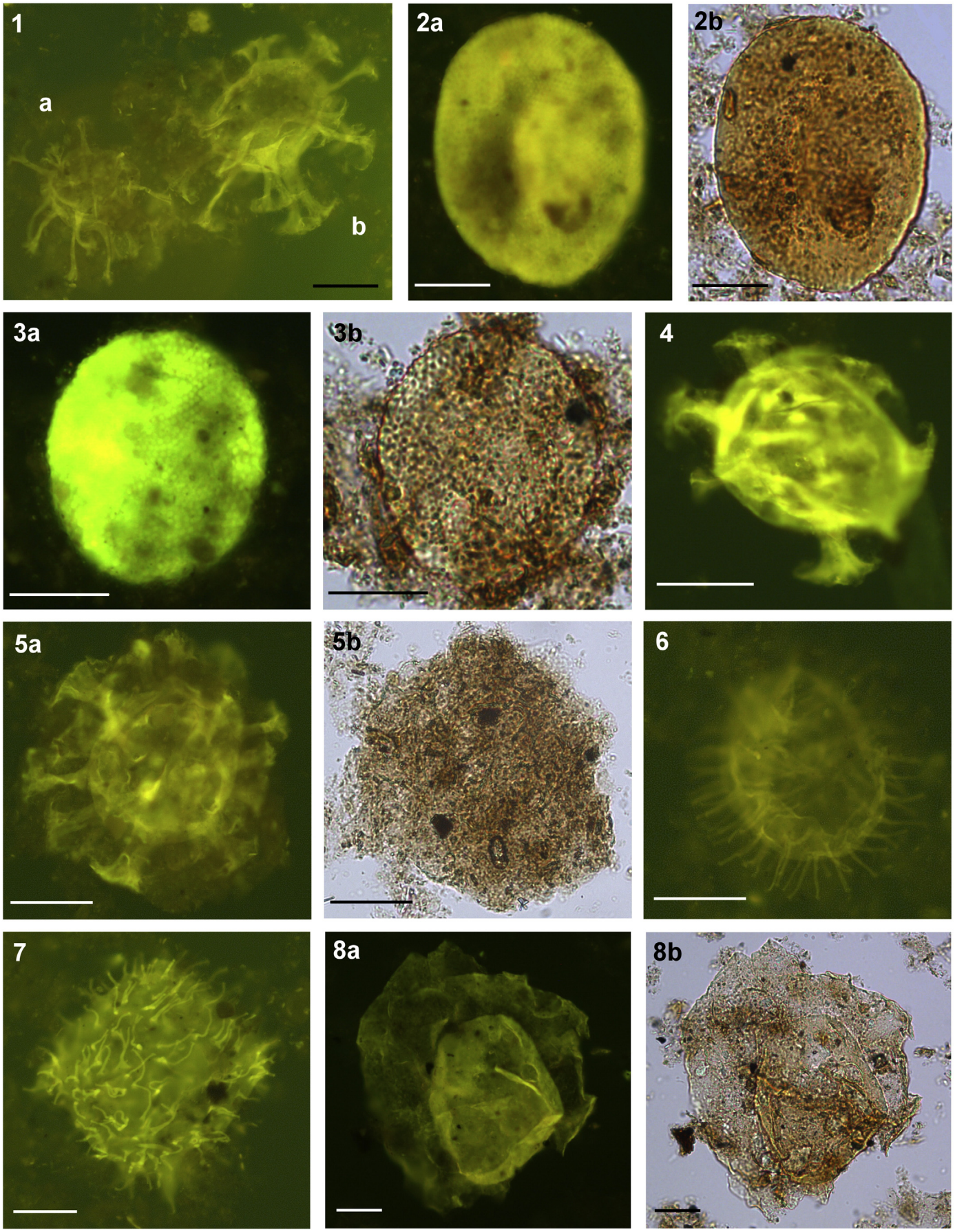

Plate I

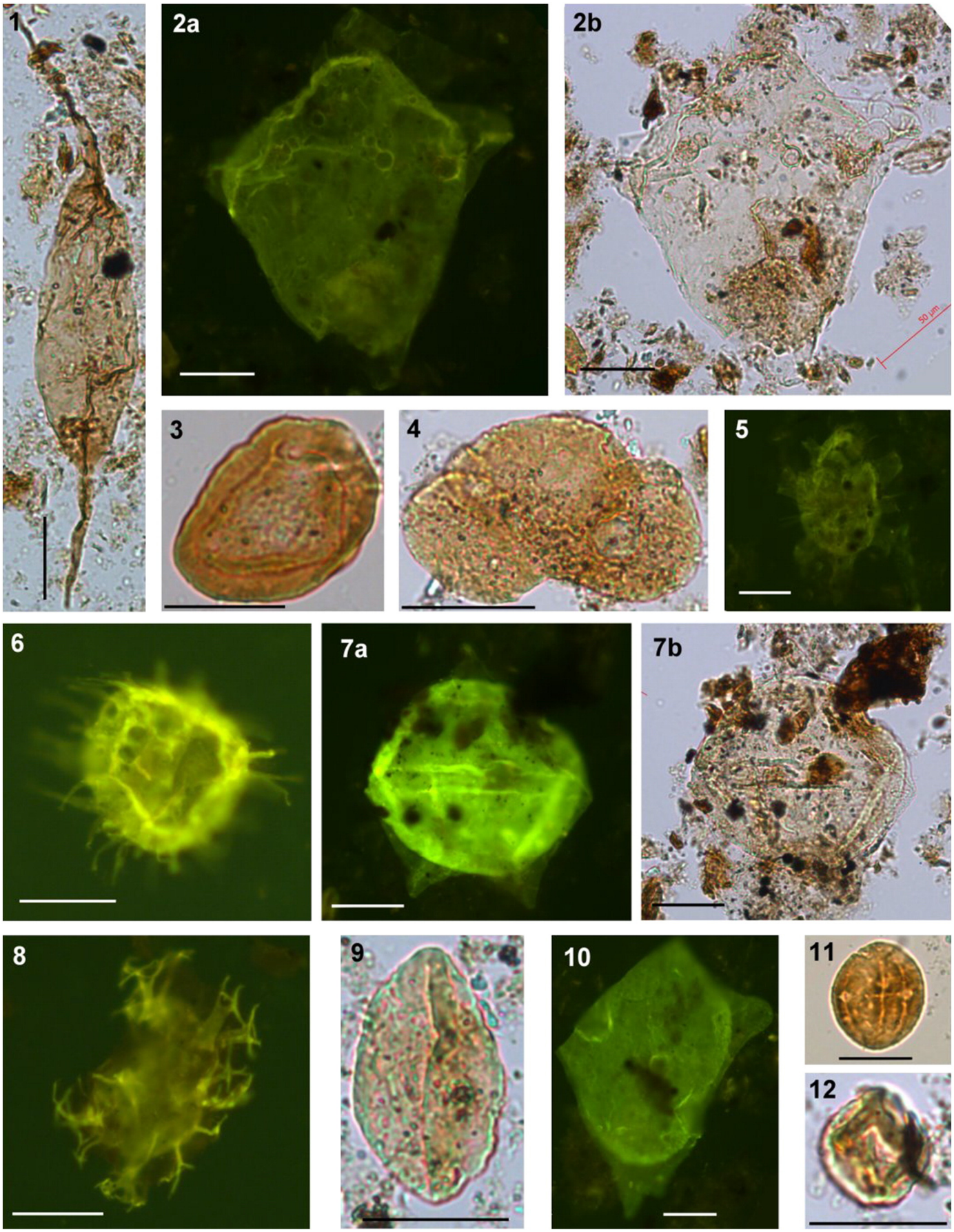

Plate II *(caption on page 10).*

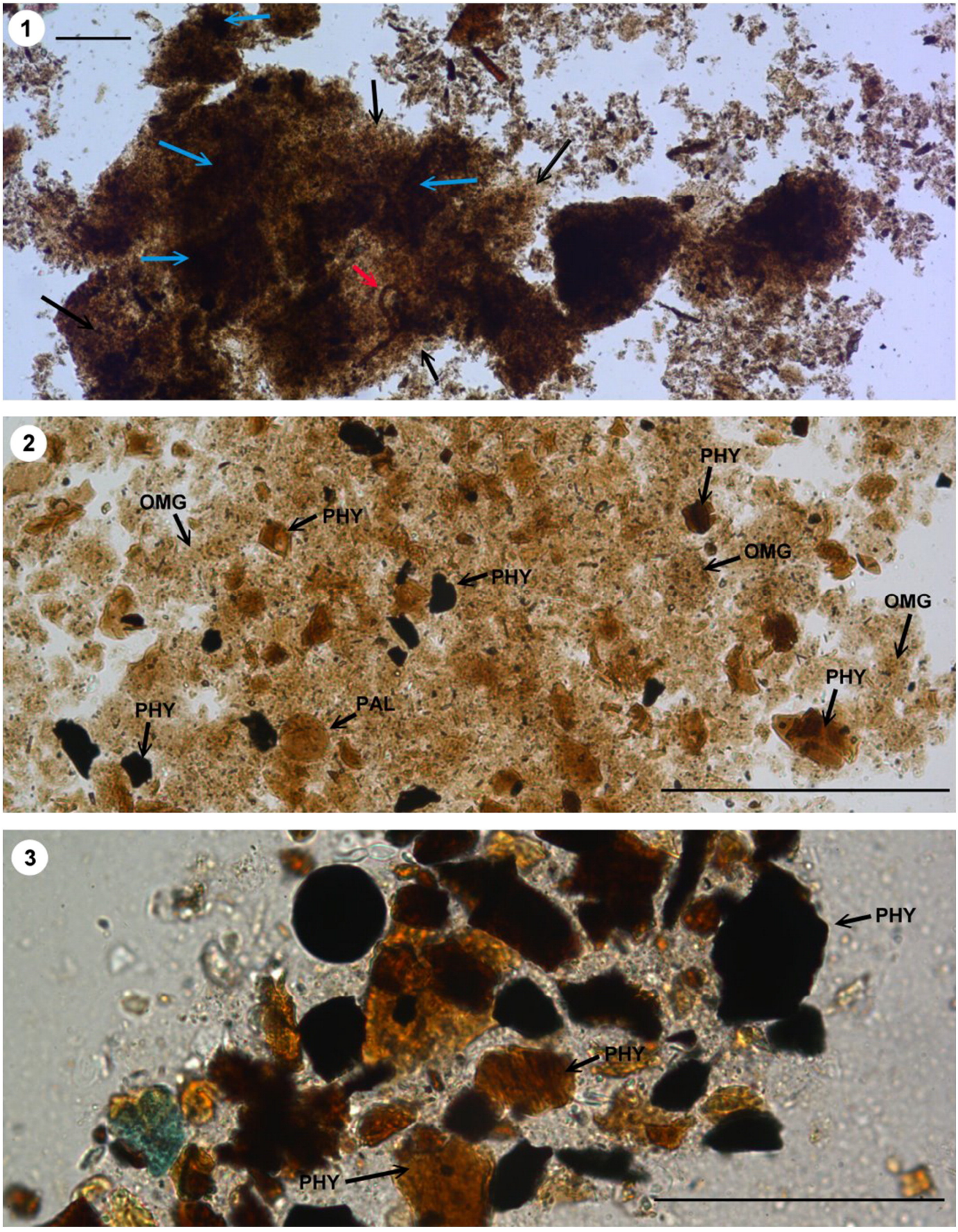

Plate III *(caption on page 10).*

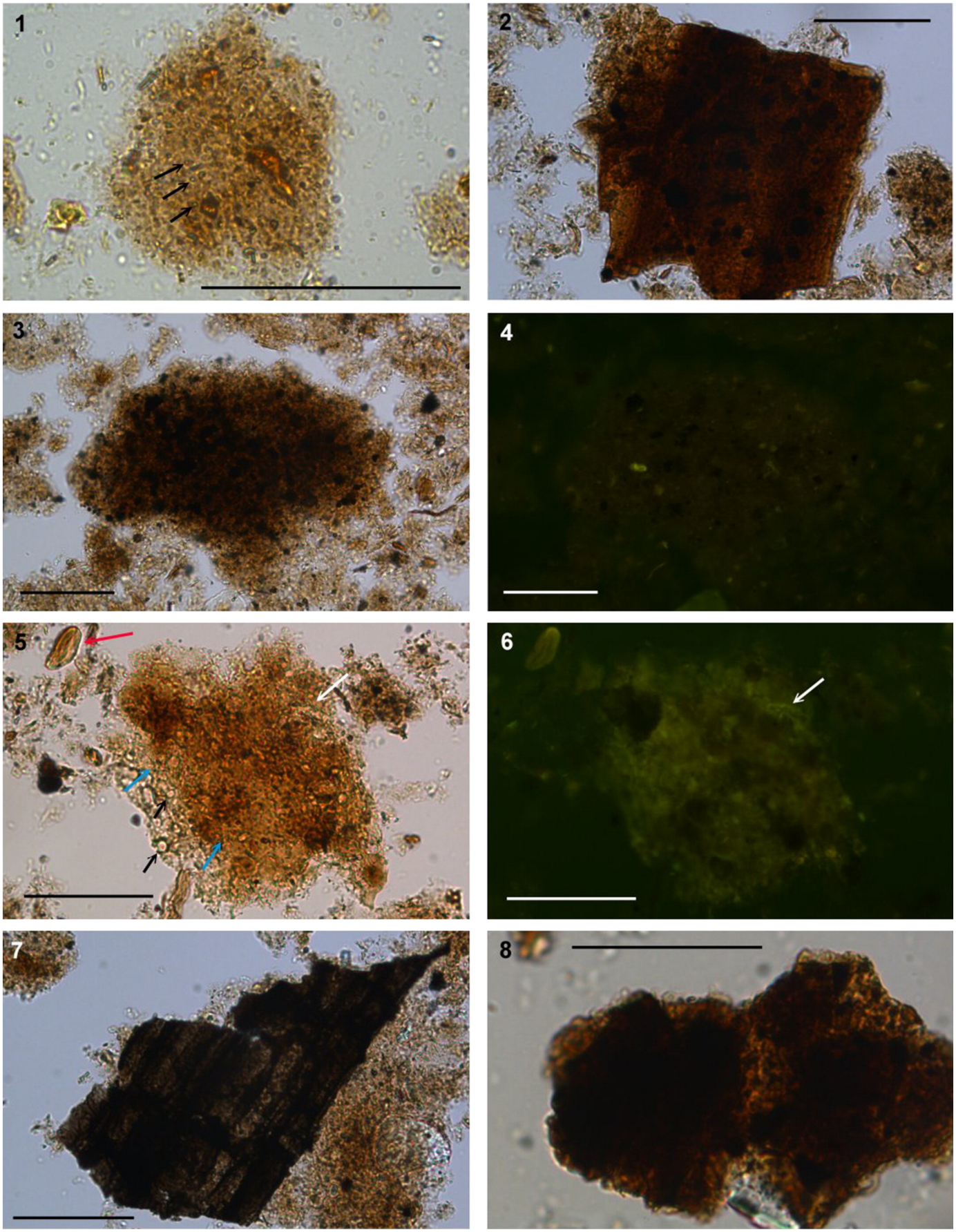

Plate IV *(caption on page 10).*

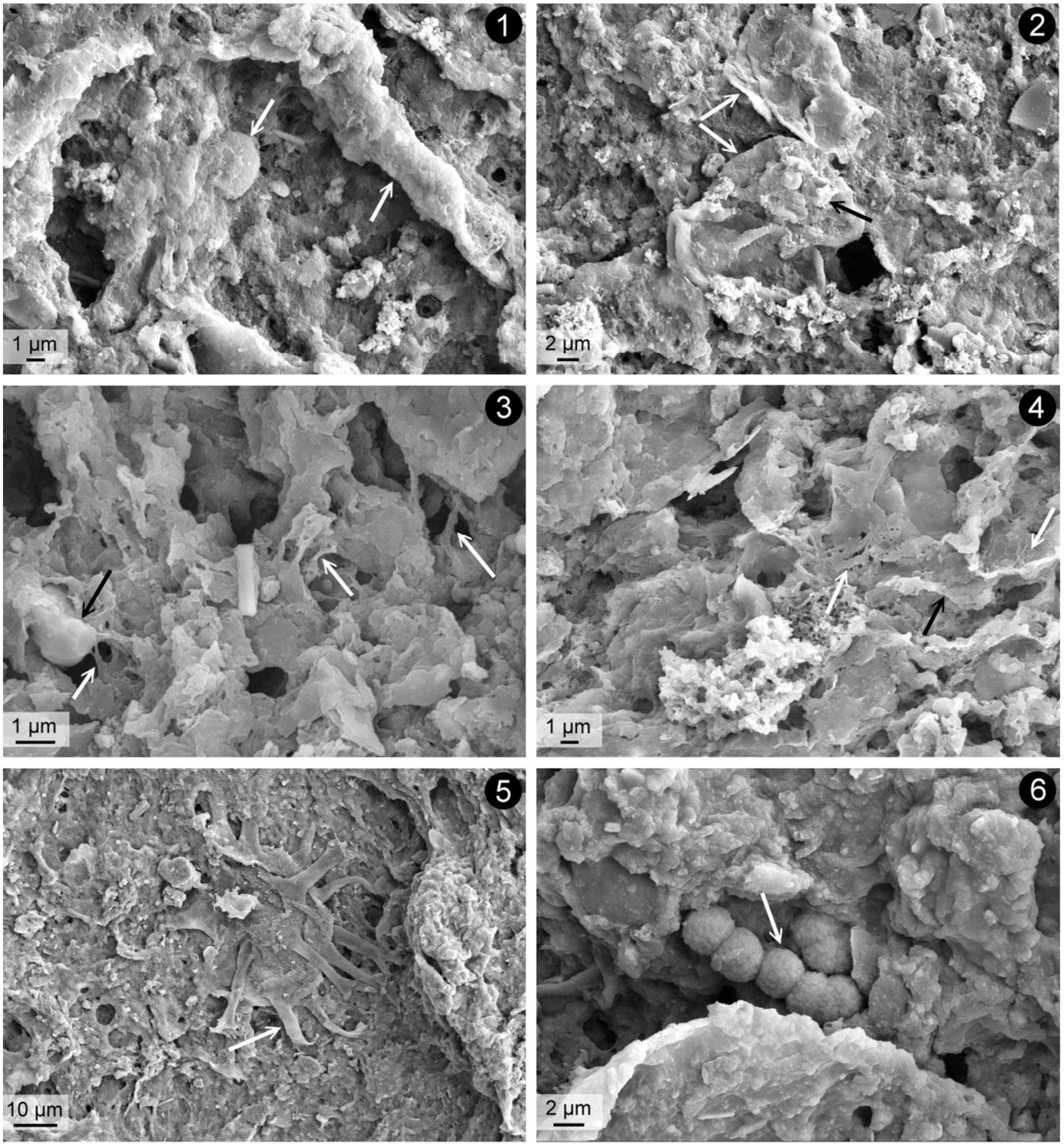

Plate V. SEM images of the palynofacies assemblage PF-1 showing: 1. coccoid and filamentous bacteria (arrows) from the Piatra Pinului section, Lower Dysodilic Shale Formation; 2. algae (white arrows) covered by EPS (black arrow) from the Piatra Pinului section, Lower Dysodilic Shale Formation; 3. coccoid bacteria (black arrow) embedded into EPS (white arrows) from the Domnişoara section, Lower Dysodilic Shale Formation; 4. a terrestrial fragment (black arrow) covered by EPS (white arrows) from the Domnişoara section, Lower Dysodilic Shale Formation; 5. an intact dinoflagellate with processes (arrow) from the Frasin section, Lower Dysodilic Shale Formation; 6. a colony of coccoid bacteria (arrow) from the Frasin section, Lower Dysodilic Shale Formation.

The T_{max} values vary between 419° and 429 °C, suggesting slightly mature organic matter. As illustrated in the HI vs. T_{max} diagram (Fig. 5A; from Espitalié et al., 1985), the organic matter is attributed to kerogen type II (oil prone) and would be expected to expel mostly mixed oil and gas (Fig. 5B).

The Lower Dysodilic Shale Formation cropping out in the Domnişoara (LS4) and Frasin (LS2) sections displays a hydrocarbon potential between good and excellent (Table 1), the thermal maturity of kerogen (based on TAI and fluorescence) being at the limit between immature and mature (Fig. 2). Based on optical criteria, the kerogen

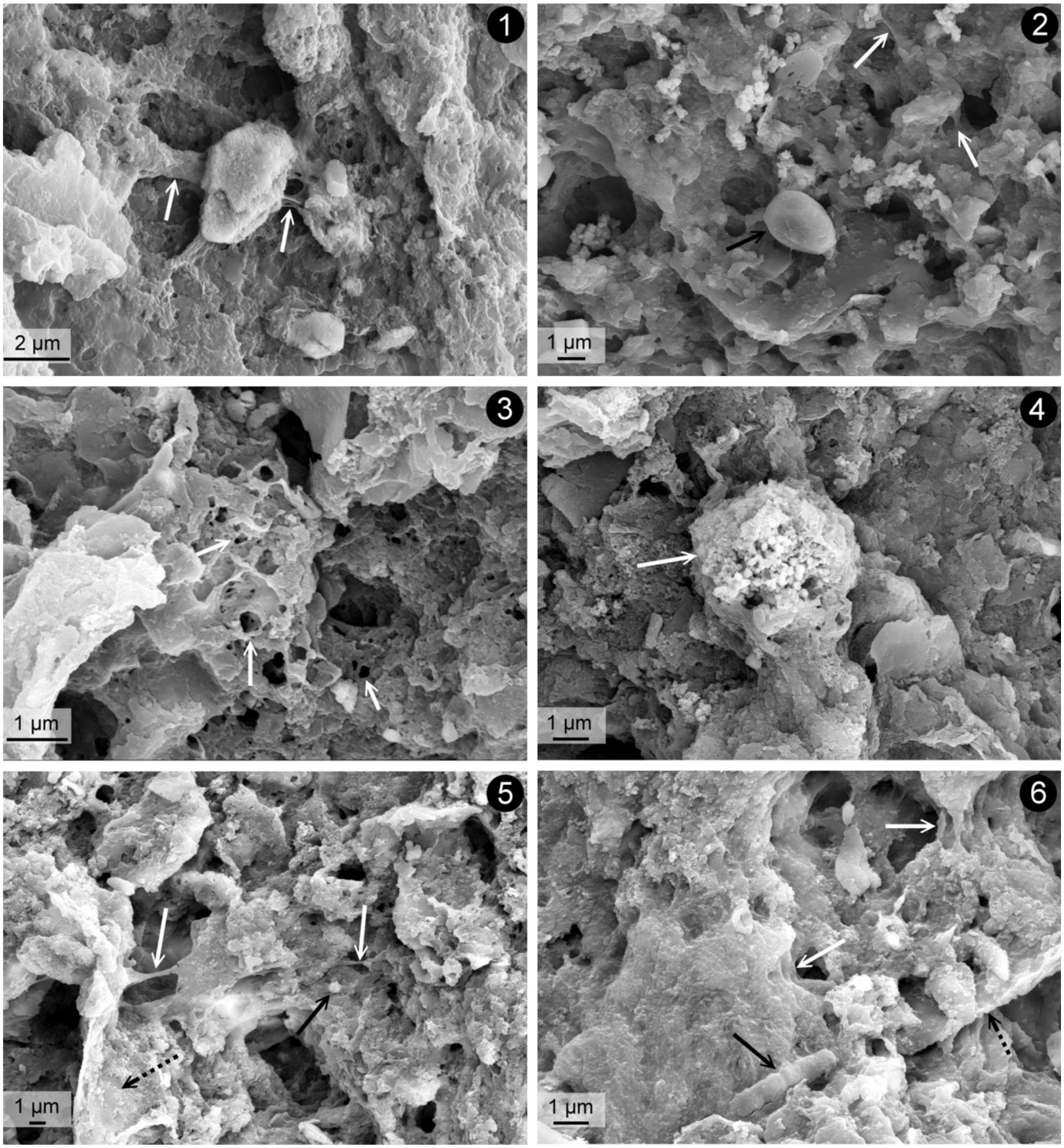

Plate VI. SEM images of the palynofacies assemblage PF-1 (1–4) and PF-2 (5, 6) showing: 1. abundant EPS (arrows) embedding non identifiable organic particles from the Slănic section, Lower Dysodilic Shale Formation; 2. isolated coccoid bacteria (black arrow) and abundant EPS (white arrows) from the Slănic section, Lower Dysodilic Shale Formation; 3. abundant EPS characterized by an alveolar network (arrows) from the Dumesnic section, Lower Dysodilic Shale Formation; 4. framboidal pyrite (arrow) from the Dumesnic section, Lower Dysodilic Shale Formation; 5. a membrane (dashed arrow) colonized by a biofilm, i.e., bacteria (black arrow) and EPS (white arrows) from the Piatra Pinului section, Upper Dysodilic Shale Formation; 6. an unidentifiable organic particle (dashed arrow) covered by EPS (white arrows) embedding a bacterium in the cellular division process (black arrow), from the Piatra Pinului section, Upper Dysodilic Shale Formation.

may be type II, with an abundance of granular AOM and prasinophyte algae, dinocysts and pollen.

From the Piatra Pinului outcrop (LS1), the Bituminous Marls Formation and the Lower Dysodilic Shale Formation have TOC values ranging from 2 to 9% (Table 1), their potential being very good to excellent. The visual determination of palynomorph color produced a TAI between 2 and 2+, indicating the limit between immature and mature stages of hydrocarbon generation. The fluorescence color of prasinophyte algae

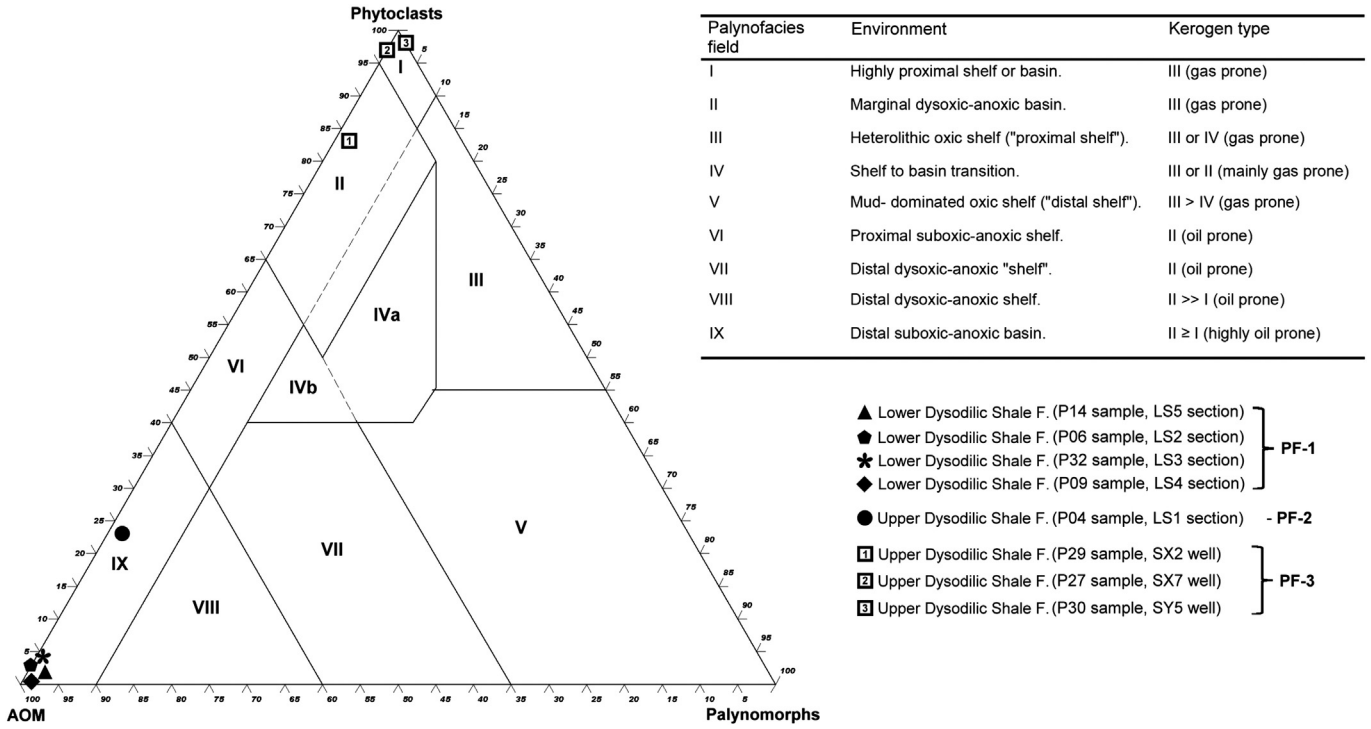

Palynofacies field	Environment	Kerogen type
I	Highly proximal shelf or basin.	III (gas prone)
II	Marginal dysoxic-anoxic basin.	III (gas prone)
III	Heterolithic oxic shelf ("proximal shelf").	III or IV (gas prone)
IV	Shelf to basin transition.	III or II (mainly gas prone)
V	Mud- dominated oxic shelf ("distal shelf").	III > IV (gas prone)
VI	Proximal suboxic-anoxic shelf.	II (oil prone)
VII	Distal dysoxic-anoxic "shelf".	II (oil prone)
VIII	Distal dysoxic-anoxic shelf.	II >> I (oil prone)
IX	Distal suboxic-anoxic basin.	II ≥ I (highly oil prone)

▲ Lower Dysodilic Shale F. (P14 sample, LS5 section)
⬟ Lower Dysodilic Shale F. (P06 sample, LS2 section)
★ Lower Dysodilic Shale F. (P32 sample, LS3 section)
◆ Lower Dysodilic Shale F. (P09 sample, LS4 section) — PF-1
● Upper Dysodilic Shale F. (P04 sample, LS1 section) — PF-2
1 Upper Dysodilic Shale F. (P29 sample, SX2 well)
2 Upper Dysodilic Shale F. (P27 sample, SX7 well)
3 Upper Dysodilic Shale F. (P30 sample, SY5 well) — PF-3

Fig. 4. Ternary kerogen plots (Tyson, 1995) for the Lower and Upper Dysodilic Shale Formations (PF-1 to PF-3 palynofacies types), indicating deposition in a distal suboxic-anoxic basin for PF-1 and PF-2, and a marginal dysoxic-anoxic basin for PF-3.

is golden yellow-green, suggesting a vitrinite reflectance (VRo) of up to 0.7%. The kerogen is type II (oil prone), based on geochemical criteria (H/C and O/C ratios, plotted in a Van Krevelen diagram; Fig. 5D). In palynological slides, the kerogen is predominantly in granular and rarely gelified AOM, phytoplankton and EPS.

The Upper Dysodilic Shale Formation analyzed in the 4 wells from the Slănic-Oituz Half-window (Vrancea Nappe) has TOC contents between 1.9 and 10%, its oil and gas potential ranging between good and excellent (Table 1). Kerogen maturity estimated from TAI exhibits values between 2 and 2+ (immature/mature stage). Optically, the organic matter may suggest a type III kerogen, abundant in translucent and opaque phytoclasts (continental source), with low amounts of AOM. This type of kerogen generates mainly gas.

In summary, the petroleum potential of the Lower Dysodilic Shale Formation is generally very good to excellent, both in the Tarcău and Vrancea Nappes. This formation contains mainly type II (oil prone) kerogen, which is at the limit between the immature and mature stages of hydrocarbon generation. The organic matter from the Upper Dysodilic Shale Formation may indicate a type III (gas prone) kerogen, with a petroleum potential ranging between good and excellent. Hydrocarbon products generated by these organic-rich black shales have migrated to petroleum reservoirs, the most important being the Kliwa Formation (Fig. 1, see lithological columns). Processes of generation–migration–accumulation of the hydrocarbons in these reservoir rocks have occurred from the middle/upper Miocene until the present (Ştefănescu et al., 2006).

5. Conclusions

Microscopic and geochemical investigations of the Oligo-Miocene bituminous rocks from the Moldavidian Domain (Lower and Upper Dysodilic Shale Formations) indicate that they are organic-rich and were deposited under suboxic to anoxic conditions, and are therefore of petroleum interest. The main conclusions reached in the present study are the following:

(1) Based on palynological assemblages, the age of the Lower Dysodilic Shale Formation is Rupelian–early Chattian (dinocysts zone D14–the lower part of D15, after Köthe and Piesker, 2007), and older than middle Aquitanian for the Upper Dysodilic Shale Formation. The age of this latter formation is suggested by *Deflandrea phosphoritica*, with the last occurrence of this taxon at the top of the DN1 zone from Germany.

(2) The Lower Dysodilic Shale Formation exhibits high phytoplankton assemblage diversity (dinoflagellate cysts and prasinophyte algae), along with subordinated pollens and spores. The abundance of continental palynomorphs increases in the Upper Dysodilic Shale Formation, with phytoplankton represented only by *Deflandrea phosphoritica* and *Tytthodiscus* sp.

(3) Three types of palynofacies were distinguished, as follows: PF-1 (Lower Dysodilic Shale Formation) is dominated by granular AOM of marine origin (derived from phytoplankton and bacteria) accumulated in O_2-depleted waters, and rarely contains gelified AOM (of terrestrial origin). The AOM displays weak fluorescence due to microbial degradation. PF-2 (the lower part of the Upper Dysodilic Shale Formation) exhibits a decrease in AOM content, while PF-3 (the middle and upper parts of the Upper Dysodilic Shale Formation) is mainly comprised of phytoclasts (terrestrial source). PF-1 and PF-2 suggest sedimentation in a distal/marginal suboxic–anoxic basin, while a highly proximal shelf setting is inferred for PF-3.

(4) Dinoflagellate taxa suggest moderate seawater salinity during deposition of the Lower Dysodilic Shale Formation, as

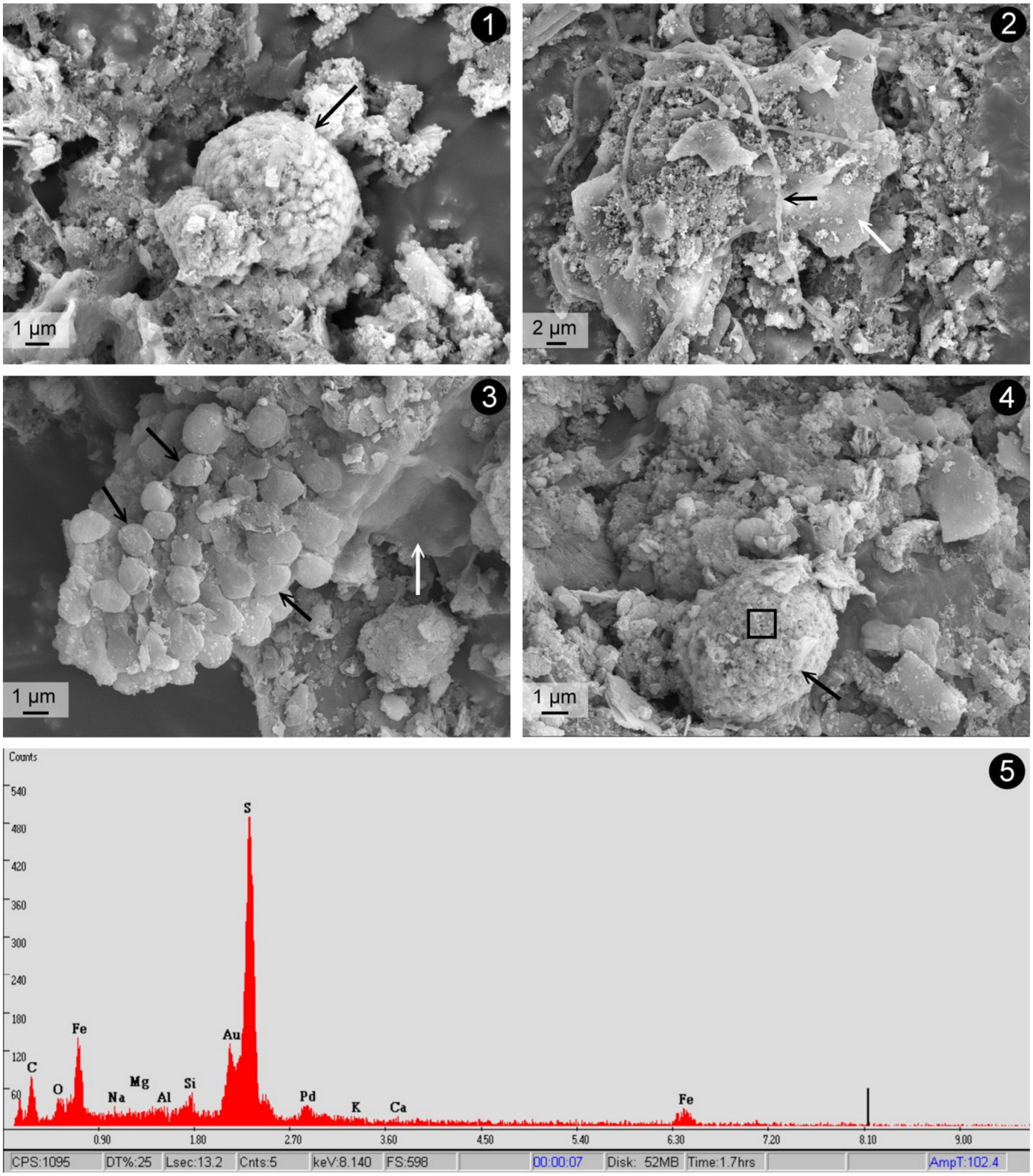

Plate VII. SEM images of the palynofacies assemblage PF-3 showing: 1. framboidal pyrite (arrow) from the SX2 well, Upper Dysodilic Shale Formation; 2. a terrestrial fragment in an early degradation stage, i.e., intact shape (white arrow) covered by filamentous bacteria (black arrow), from the SX2 well, Upper Dysodilic Shale Formation; 3. a colony of coccoid bacteria (black arrows) associated with EPS (white arrow) from the SY5 well, Upper Dysodilic Shale Formation; 4. framboidal pyrite (arrow) from the SY5 well, Upper Dysodilic Shale Formation; 5. associated elemental analysis using EDAX (see square in image 4).

shown by the presence of *Homotryblium* div. sp. and *Operculodinium centrocarpum*. The growth waters were warm temperate to tropical (*Homotryblium* and *Spiniferites ramosus*) and O_2-depleted (*Thalassiphora pelagica*). Dinocyst assemblages (r, *Deflandrea*, *Lingulodinium machaerophorum*, *Rhombodinium* and *Wetzeliella*) in both the Lower and

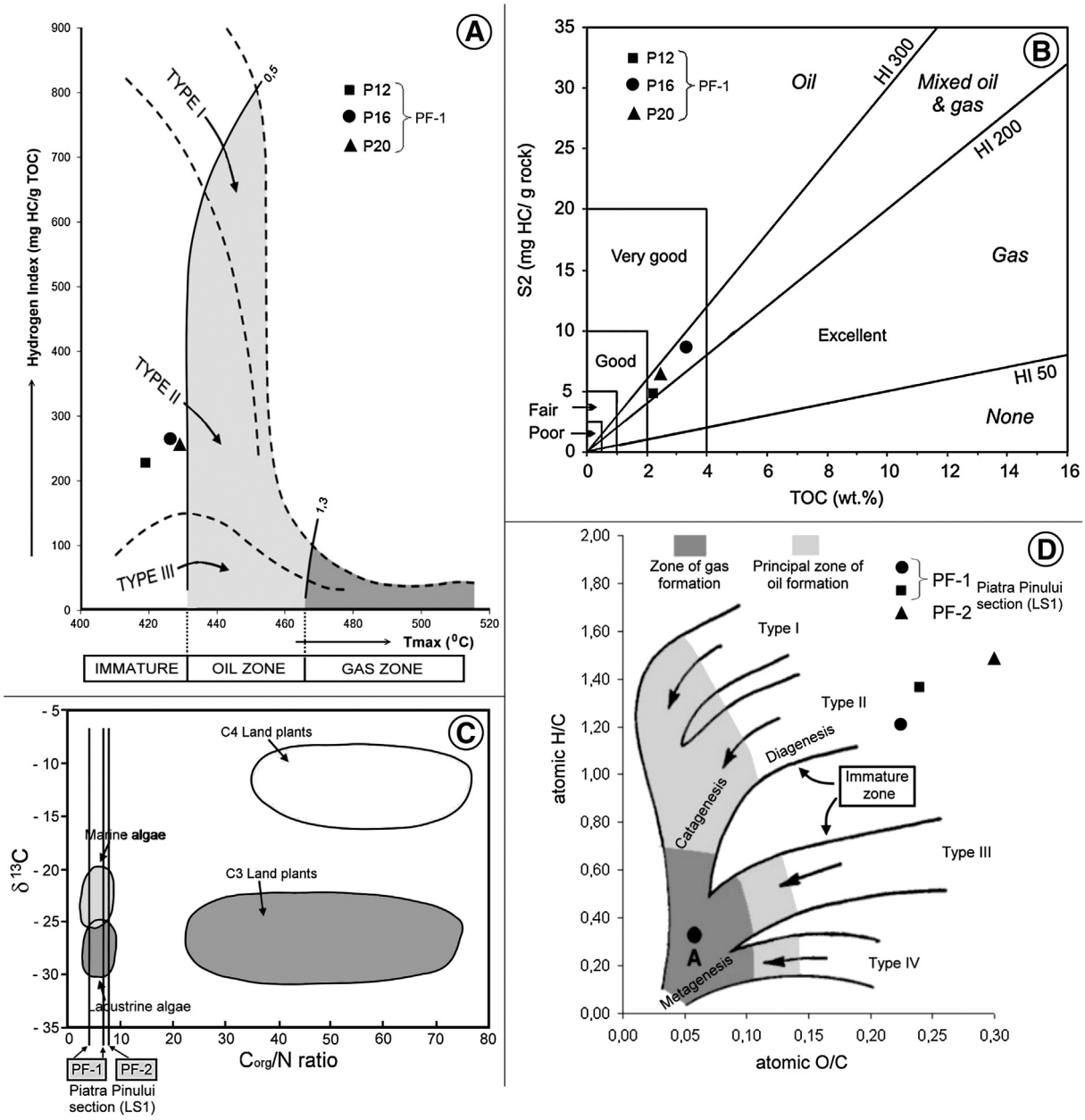

Fig. 5. Plots of (A) HI vs. T_{max}, (B) S_2 vs. TOC, (C) C_{org}/N (Meyers, 1994) and (D) the H/C and O/C atomic ratios for some of the analyzed samples, depicting kerogen type, petroleum potential and the main products expected to be expelled at peak maturity, as well organic matter source (continental or marine). The classifications of petroleum potential and expelled products are those of Peters and Cassa (1994).

Upper Dysodilic Shale Formations imply nutrient-rich waters. The continentally derived palynomorphs suggest swamp, lowland riparian, and mixed mesophytic forest environments, as well as high altitude source areas.

(5) The palynological and geochemical analyses conducted on kerogen may indicate that the Lower Dysodilic Shale Formation (Tarcău and Vrancea Nappes) is oil-prone, type II, and is mainly composed of granular AOM of microbial and phytoplanktonic origin. The Upper Dysodilic Shale Formation, on the other hand, may contain gas-prone, type III kerogen. Both types of kerogen are slightly mature, with potential for hydrocarbon generation. Therefore, both the Lower and the Upper Dysodilic Shale Formations are of particular interest for petroleum exploration.

Acknowledgments

The authors wish to express their gratitude towards the University of Zurich for providing the SEM facilities. Many thanks to our colleagues Sandu Marius Cristian (Geolog International Company), for his help with the Rock-Eval analyses, and Stoicescu Alexandru (Petrom Company) for the core samples provided. We are also grateful to the anonymous reviewers for their comments and suggestions, which greatly improved the earlier version of this manuscript.

Appendix 1. Taxonomic list of palynomorphs identified in the Tarcău and Vrancea Nappes

Taxa	Tarcău Nappe	Vrancea Nappe	
	Lower Dysodilic Shale F. (%)	Lower Dysodilic Shale F. (%)	Upper Dysodilic Shale F. (%)
Phytoplankton			
Achomosphaera ramulifera (Deflandre 1937) Evitt, 1963		1.6	
Achomosphaera sp.	0.9		
Cordosphaeridium gracile (Eisenack 1954) Davey and Williams, 1966	0.9	3.2	
Cordosphaeridium inodes (Klumpp 1953) Eisenack, 1963	0.9	1.6	
Cordosphaeridium sp.	2.8		
Deflandrea phosphoritica Eisenack, 1938	6.6	11.3	4.5
Deflandrea sp.	2.8	3.2	
Dracodinium sp. (reworking)		1.6	
Homotryblium plectilum Drugg and Loeblich Jr, 1967	4.7	11.3	
Homotryblium aculeatum Williams, 1978		3.2	
Homotryblium vallum Stover, 1977		1.6	
Homotryblium sp.	0.9	1.6	
Hystrichokolpoma rigaudiae Deflandre and Cookson, 1955	1.9	1.6	
Lingulodinium pycnospinosum (Benedek 1972) Stover and Evitt, 1978	0.9		
Lingulodinium machaerophorum (Deflandre and Cookson, 1955) Wall, 1967	0.9	1.6	
Operculodinium centrocarpum (Deflandre and Cookson, 1955) Wall, 1967	4.7	6.5	
Operculodinium sp.	0.9	1.6	
Oligosphaeridium sp.		1.6	
Palaeocystodinium golzowense Alberti, 1961	0.9		
Polysphaeridium subtile Davey and Williams, 1966	0.9	1.6	
Rhombodinium draco Gocht, 1955	4.7		
Rhombodinium perforatum (Jan du Chêne and Châteauneuf 1975) Lentin and Williams, 1977 (reworking)	1.9		
Rhombodinium sp.	1.9		
Spiniferites ramosus (Ehrenberg 1838) Mantell 1854	1.9	3.2	
Spiniferites sp.	1.9	1.6	
Thalassiphora pelagica (Eisenack 1954) Eisenack and Gocht, 1960	7.5	9.7	
Thalassiphora sp.	0.9		
Tytthodiscus sp.	20.8	4.8	31.8
Wetzeliella gochtii Costa and Downie, 1976	0.9		
Wetzeliella sp.	0.9		
Pollen and spores			
Leiotriletes sp.		1.6	
Osmunda sp.			4.5
Polypodiaceoisporites sp.			9.1
Verrucatosporites sp.	0.9		
Abiespollenites sp.		1.6	
Pityosporites sp.	13.2	4.8	13.6
Pityosporites microalatus (Potonié 1931) Thomson and Pflug, 1953	2.8	9.7	
Pityosporites insignis (Naumova ex Bolchovitina 1953) Krutzsch, 1971	0.9		
Pityosporites labdacus (Potonié 1931) Thomson and Pflug, 1953	0.9		
Sciadopityspollenites sp.		1.6	
Taxodium sp.	1.9	4.8	9.1
Corylus sp.	0.9		
Cyrillaceaepollenites exactus (Potonié 1931) Potonié, 1960	0.9		
Engelhardia sp.			4.5
Monocolpopollenites tranquillus (Potonié 1934) Thomson and Pflug, 1953	0.9		
Myrica sp.			9.1
Quercus sp.			4.5
Sapotaceoidaepollenites sp.			4.5
Tricolporopollenites microhenrici (Potonié 1931) Krutzsch, 1961			4.5
Ulmus sp.	0.9		

References

Alberti, G., 1961. Zur Kenntnis mesozoischer und alttertiärer Dinoflagellaten und Hystrichosphaerideen von Nord- und Mitteldeutschland sowie einigen anderen europäischen Gebieten. Palaeontogr. Abt. A 116, 1–58.

Amadori, M.L., Belayouni, H., Guerrera, F., Martín-Martín, M., Martin-Rojas, I., Miclăuş, C., Raffaelli, G., 2012. New data on the Vrancea Nappe (Moldavidian Basin, Outer Carpathian Domain, Romania): paleogeographic and geodynamic reconstructions. Int. J. Earth Sci. (Geol. Rundsch.) 101, 1599–1623.

Bădescu, D., 2005. Evoluţia tectono-stratigrafică a Carpaţilor Orientali în decursul Mezozoicului şi Neozoicului. Editura Economică, Bucureşti (312 pp.).

Balteş, N., 1969. Distribution stratigraphique des dinoflagellés et des acritarches tertiaires en Roumanie. In: Brönnimann, P., Renz, H.H. (Eds.), 1st International Conference on Planktonic Microfossils, Geneva, 1967, Proceedings. v.1, pp. 26–45.

Balteş, N., 1983. Hydrocarbon source-rocks in Romania. Anu. Inst. Geol. Geofiz. Tectonică, Petrol. Gaz. LX, 265–270.

Băncilă, I., 1958. Geologia Carpaţilor Orientali. Editura Ştiinţifică, Bucureşti (368 pp.).

Barski, M., Bojanowski, M., 2010. Organic-walled dinoflagellate cysts as a tool to recognize carbonate concretions: an example from Oligocene flysch deposits of the Western Carpathians. Geol. Carpath. 61 (2), 121–128.

Batten, D.J., 1983. Identification of amorphous sedimentary organic matter by transmitted light microscopy. In: Brooks, J. (Ed.), Petroleum Geochemistry and Exploration of Europe: Boston. The Geological Society Special Publication 12. Blackwell Scientific Publications, pp. 275–287.

Batten, D.J., 1999. Small palynomorphs. In: Jones, T.P., Rowe, N.P. (Eds.), Fossil Plants and Spores: Modern Techniques. Geological Society, London, pp. 15–19.

Belayouni, H., Di Staso, A., Guererra, F., Martin, M.M., Miclăuş, C., Serrano, F., Tramontana, M., 2009. Stratigraphic and geochemical study of the organic-rich black shales in the Tarcău Nappe of the Moldavidian Domain (Carpathian Chain, Romania). Int. J. Earth Sci. 98, 157–176.

Bombardiere, L., Gorin, G.E., 2000. Stratigraphical and lateral distribution of sedimentary organic matter in Upper Jurassic carbonates of SE France. Sediment. Geol. 132, 177–203.

Candel, M.S., Radi, T., de Vernal, A., Bujalesky, G., 2012. Distribution of dinoflagellate cysts and other aquatic palynomorphs in surface sediments from the Beagle Channel, Southern Argentina. Mar. Micropaleontol. 96–97, 1–12.

Carvalho, M.A., Mendonça Filho, J.G., Menezes, T.R., 2006. Palynofacies and sequence stratigraphy of the Aptian–Albian of the Sergipe Basin, Brazil. Sediment. Geol. 192, 57–74.

Charles, J.J., 2009. Image analysis of microscope slides for palynofacies studies. (Ph.D. Thesis), Bangor University, UK (172 pp.).

Combaz, A., 1980. Les kérogenes vus au microscope. In: Durand, B. (Ed.), Kerogen. Insoluble organic matter from sedimentary rocks. Editions Technip, Paris, pp. 55–113.
Costa, L.I., Downie, C., 1976. The distribution of the dinoflagellate *Wetzeliella* in the Palaeogene of north-western Europe. Palaeontology 19, 591–614.
Courtinat, B., Hantzpergue, P., Rio, M., Mazin, J.M., 2003. Sedimentary organic matter and palaeoenvironments in the Lower Tithonian of the Quercy (France). Geobios 36, 13–25.
Davey, R.J., Williams, G.L., 1966. The genus *Hystrichosphaeridium* and its allies. In: Davey, R.J., Downie, C., Sarjeant, W.A.S., Williams, G.L. (Eds.), Studies on Mesozoic and Cainozoic dinoflagellate cysts. British Museum (Natural History) Geology, Bulletin, Supplement 3, pp. 53–106.
de Vernal, A., Goyette, C., Rodrigues, C.G., 1989. Contribution palynostratigraphique (dinokystes, pollen et spores) à la connaissance de la Mer Champlain: coupe de Saint-Césaire, Québec. Can. J. Earth Sci. 26, 2450–2464.
de Verteuil, L., Norris, G., 1996. Middle to upper Miocene *Geonettia clineae*, an opportunistic coastal embayment dinoflagellate of the *Homotryblium* complex. Micropaleontology 42, 263–284.
Deflandre, G., Cookson, I.C., 1955. Fossil microplankton from Australian Late Mesozoic and Tertiary sediments. Aust. J. Mar. Freshwat. Res. 6 (2), 242–313.
Drugg, W.S., Loeblich Jr., A.R., 1967. Some Eocene and Oligocene phytoplankton from the Gulf Coast, USA. Tulane Stud. Geol. 5, 181–194.
Dumitrescu, I., Mirăuţă, O., Săndulescu, M., Ştefănescu, M., Bandrabur, T., 1968. Harta geologică a României (scara 1 :200000), foaia 21 Bacău. Institutul de Geologie şi Geofizică, Bucureşti.
Durand, B., Nicaise, G., 1980. Procedures of kerogen isolation. In: Durand, B. (Ed.), Kerogen. Insoluble Organic Matter from Sedimentary Rocks. Editions Technip, Paris, pp. 35–53.
Dybkjær, K., Piasecki, S., 2010. Neogene dinocyst zonation for the eastern North Sea Basin, Denmark. Rev. Palaeobot. Palynol. 161, 1–29.
Eisenack, A., 1938. Die Phosphoritknollen der Bernsteinformation als Überlieferer tertiären Planktons. Schriften der Physikalisch-Ökonomischen Gesellschaft zu Königsberg 70 (2), 181–188.
Eisenack, A., 1963. *Cordosphaeridium* n.g., ex *Hystrichosphaeridium*, Hystrichosphaeridea. Neues Jb. Geol. Paläontol. Abh. 118, 260–265.
Eisenack, A., Gocht, H., 1960. Neue Namen für einige Hystrichosphären der Bernsteinformation Ostpreussens. Neues Jb. Geol. Paläontol. Monat. 11, 511–518.
Ekpo, B.O., Essien, N., Fubara, E.P., Ibok, U.J., Ukpabio, E.J., Wehner, H., 2013. Petroleum geochemistry of Cretaceous outcrops from the Calabar Flank, southeastern Nigeria. Mar. Pet. Geol. 48, 171–185.
Ercegovac, M., Kostić, A., 2006. Organic facies and palynofacies: nomenclature, classification and applicability for petroleum source rock evaluation. Int. J. Coal Geol. 68, 70–78.
Espitalié, J., Deroo, G., Marquis, F., 1985. La pyrolyse Rock Eval et ses applications (deuxième partie). Rev. Inst. Fr. Pétrol. 40, 755–784.
Evitt, W.R., 1963. A discussion and proposals concerning fossil dinoflagellates, hystrichospheres, and acritarchs, I. Natl. Acad. Sci. Wash. Proc. 49, 158–164.
Gedl, P., 2005. Late Eocene–early Oligocene organic-walled dinoflagellate cysts from Folusz, Magura Nappe, Polish Carpathians. Acta Palaeobot. 45 (1), 27–83.
Gerlach, E., 1961. Mikrofossilien aus dem Oligozän und Miozän Nordwestdeutschlands, unter besonderer Berücksichtigung der Hystrichosphaeren und Dinoflagellaten. Neues Jb. Geol. Paläontol. Abh. 112 (2), 143–228.
Gocht, H., 1955. *Rhombodinium* und *Dracodinium*, zwei neue Dinoflagellaten-Gattungen aus dem norddeutschen Tertiär. Neues Jb. Geol. Paläontol. Monat. 2, 84–92.
Götz, A.E., Feist-Burkhardt, S., Ruckwied, K., 2008. Palynofacies and sea-level changes in the Upper Cretaceous of the Vocontian Basin, southeast France. Cretac. Res. 29, 1047–1057.
Grasu, C., Catană, C., 1989. Variations chimico-mineralogiques et de contenu en matiere organique des dysodiles oligocenes a travers de flysch carpatique. The Oligocene from the Transylvanian Basin, Special issues, Cluj-Napoca 363–369.
Grasu, C., Catană, C., Grinea, D., Ionesi, L., 1976. Consideraţii geologice şi geochimice asupra rocilor bituminoase oligocene din zona cuprinsă între pârâul Cuejdiu şi Ozana. Anu. Muz. Ştiinţe Nat. III 65–99.
Grasu, C., Catană, C., Grinea, D., 1988. Flişul carpatic. Petrografie şi consideraţii economice. Editura Tehnică, Bucureşti (208 pp.).
Grasu, C., Catană, C., Miclăuş, C., Boboş, I., 1999. Molasa Carpaţilor Orientali, petrografie şi sedimentogeneză. Editura Tehnică, Bucureşti (227 pp.).
Grasu, C., Miclăuş, C., Florea, F., Şaramet, M., 2007. Geologia şi valorificarea economică a rocilor bituminoase din România. Editura Universităţii "Al. I. Cuza", Iaşi (253 pp.).
Harland, R., 1983. Distribution maps of recent dinoflagellate cysts in bottom sediments from the North Atlantic Ocean and adjacent seas. Palaeontology 26, 321–387.
Iakovleva, A.I., 2011. Palynological reconstruction of the Eocene marine palaeoenvironments in south of Western Siberia. Acta Palaeobot. 51 (2), 229–248.
Ionesi, L., 1971. Flişul paleogen din bazinul văii Moldovei. Editura Academiei, Bucureşti (250 pp.).
Islam, M.A., 1984. A study of Early Eocene palaeoenvironments in the Isle of Sheppey as determined from microplankton assemblage composition. Tertiary Res. 6, 11–21.
Köthe, A., 1990. Paleogene dinoflagellates from Northwest Germany. Geol. Jahrb. Reihe A 118, 111.
Köthe, A., 2003. Dinozysten-Zonierung im Tertiär Norddeutschlands. Rev. Paléobiol. 22 (2), 895–923.
Köthe, A., 2005. Korrelation der Dinozysten-Zonen mit anderen biostratigraphisch wichtigen Zonierungen im Tertiär Norddeutschlands. Rev. Paléobiol. 24 (2), 697–718.
Köthe, A., Piesker, B., 2007. Stratigraphic distribution of Paleogene and Miocene dinocysts in Germany. Rev. Paléobiol. 26 (1), 1–39.
Krutzsch, W., 1959. Mikropaläontologische (sporenpaläontologische) Untersuchungen in der Braunkohle des Geiseltales. Geologie 21–22, 1–425.
Krutzsch, W., 1961. Beitrag zur Sporenpaläontologie der präoberoligozänen kontinentalen und marinen Tertiärablagerungen Brandenburgs. Ber. Geol. Ges. 7 (4), 29–343.
Krutzsch, W., 1971. Atlas der mittel- und jungtertiaren dispersen Sporen- und Pollensowie der Mikroplanktonformen des nordlichen Mitteleuropas. VI. VEB Gustav Fischer Verlag, Jena (234 pp.).
Lentin, J.K., Williams, G.L., 1977. Fossil dinoflagellates: index to genera and species, 1977 edition. Bedford Institute of Oceanography, Report Series, no.BI-R-77-8 (209 pp.).
Marret, F., Zonneveld, K.A.F., 2003. Atlas of modern organic-walled dinoflagellate cyst distribution. Rev. Palaeobot. Palynol. 125, 1–200.
Masran, T.C., Pocock, S.A.J., 1981. The classification of plant-derived particulate organic matter in sedimentary rocks. In: Brooks, J. (Ed.), Academic Press, London, pp. 145–176.
Mendonça Filho, J.G., Carvalho, M.A., Menezes, T.R., 2002. Palinofácies. In: Dutra, T.L. (Ed.), Técnicas e Procedimentos para o Trabalho com Fósseis e Formas Modernas Comparativas. Unisinos, São Leopoldo, pp. 20–24.
Mendonça Filho, J.G., Menezes, T.R., Oliveira Mendonça, J., Donizeti de Oliveira, A., Freitas da Silva, T., Rondon, N.F., Sobrinho da Silva, F., 2012. Organic facies: palynofacies and organic geochemistry approaches. In: Panagiotaras, D. (Ed.), Geochemistry - Earth's System Processes. Editions InTech, pp. 211–248.
Meyers, P.A., 1994. Preservation of elemental and isotopic source identification of sedimentary organic matter. Chem. Geol. 114, 289–302.
Micu, M., 1976. Harta geologică a României (scara 1:50000), foaia 48b Piatra Neamţ. Institutul de Geologie şi Geofizică, Bucureşti.
Nacu, D., Botez, C., Ionesi, L., Voiculescu, N., 1970. Unele aspecte privind geochimia materiei organice în rocile bituminoase din bazinul văii Humorului. Stud. Cercet. Geol. Geofizi. Geogr. Geol. 2, 15, 367–379.
Olaru, L., 1978. Cercetări asupra distribuţiei stratigrafice a microflorei în flişul paleogen dintre văile Bistriţa şi Trotuş. Inst. Géol. Géophys. Mém. XXVII, 5–111 (Bucureşti).
Pacton, M., Gorin, G.E., Vasconcelos, C., 2011. Amorphous organic matter — experimental data on formation and the role of microbes. Rev. Palaeobot. Palynol. 166 (3–4), 253–267.
Pearson, D.L., 1984. Pollen/spore color 'standard'. Phillips Petroleum Company Exploration Projects Section (reproduced in Traverse, A., 1988. Palaeopalynology, Plate 1. Unwin Hyman, Boston).
Peters, K.E., Cassa, M.R., 1994. Applied source rock geochemistry. In: Magoon, L.B., Dow, W.G. (Eds.), The Petroleum System from Source to Trap. American Association of Petroleum Geologists, Memoire 60, pp. 93–117.
Potonié, R., 1960. Synopsis der Gattungen der Sporae dispersae. III. Beih. Geol. Jahrb. 39, 1–189.
Pross, J., 2001. Paleo-oxygenation in Tertiary epeiric seas: evidence from dinoflagellate cysts. Palaeogeogr. Palaeoclimatol. Palaeoecol. 166, 369–381.
Pross, J., Schmiedl, G., 2002. Early Oligocene dinoflagellate cysts from the Upper Rhine Graben (SW Germany): paleoenvironmental and paleoclimatic implications. Mar. Micropaleontol. 45, 1–24.
Pross, J., Houben, A.J.P., van Simaeys, S., Williams, G.L., Kotthoff, U., Coccioni, R., Wilpshaar, M., Brinkhuis, H., 2010. Umbria–Marche revisited: a refined magnetostratigraphic calibration of dinoflagellate cyst events for the Oligocene of the Western Tethys. Rev. Palaeobot. Palynol. 158, 213–235.
Raynaud, J.F., Robert, P., 1976. Les méthods d'étude optique de la matière organique. Bull. Centres Rech. Pau - SNPA 10, 109–127.
Robert, P., 1985. Histoire géothermique et diagenèse organique. Bull. Centres Rech. Explor. Prod. Elf-Aquitaine Mém. 8 (345 pp.).
Săndulescu, M., 1984. Geotectonica României. Editura Tehnică, Bucureşti (336 pp.).
Selley, R.C., 1997. Elements of Petroleum Geology. Second ed. Academic Press (470 pp.).
Sluijs, A., Pross, J., Brinkhuis, H., 2005. From greenhouse to icehouse; organic-walled dinoflagellate cysts as paleoenvironmental indicators in the Paleogene. Earth Sci. Rev. 68, 281–315.
Smojić, S.B., Smajlović, J., Koch, G., Bulić, J., Trutin, M., Oreški, E., Alajbeg, A., Veseli, V., 2009. Source potential and palynofacies of Late Jurassic "Lemeš facies", Croatia. Org. Geochem. 40, 833–845.
Stănescu, V., Morariu, D.C., 1986. Oleogeneza în evoluţia tectonică majoră a bazinelor orogenice din România. Stud. Cercet. Geol. Geofiz. Geogr. Geol. 31, 143–153.
Staplin, F.L., 1969. Sedimentary organic matter, organic metamorphism, and oil and gas occurrence. Bull. Can. Petrol. Geol. 17, 47–66.
Steffen, D., Gorin, G.E., 1993. Sedimentology of organic matter in upper Tithonian–Berriasian deep sea carbonates of Southeast France: Evidence of eustatic control. In: Katz, B., Pratt, L. (Eds.), Source Rocks in a Sequence Stratigraphic Framework: American Association of Petroleum Geologists. Studies in Geology no. 37, pp. 49–65.
Stoicescu, A., 2004. Palinologia şi biostratigrafia Miocenului inferior şi a bituminelor asociate din Semifereastra Slănic - Oituz. (Ph.D. Thesis), Al. I. Cuza" University, Iaşi (163 pp.).
Stover, L.E., 1977. Oligocene and Early Miocene dinoflagellates from Atlantic Corehole 5/5B, Blake Plateau. Am. Assoc. Stratigr. Palynol. Contrib. Ser. (5A), 66–89.
Stover, L.E., Evitt, W.R., 1978. Analyses of pre-Pleistocene organic-walled dinoflagellates. Stanf. Univ. Publ. Geol. Sci. 15, 300.
Suárez-Ruiz, I., Flores, D., Mendonça Filho, J.G., Hackley, P.C., 2012. Review and update of the applications of organic petrology: Part 1, geological applications. Int. J. Coal Geol. 99, 54–112.
Ştefănescu, M., Dicea, O., Butac, A., Ciulavu, D., 2006. Hydrocarbon geology of the Romanian Carpathians, their foreland, and the Transylvanian Basin. In: Golonka, J., Picha, F.J. (Eds.), The Carphathians and their Foreland: Geology and Hydrocarbon Resources. AAPG Memoire 84, pp. 521–567.
Thomson, P.W., Pflug, H., 1953. Pollen und Sporen des mitteleuropäischen Tertiärs. Palaeontographica B 94 (1–4), 1–138.
Tissot, B.P., Welte, D.H., 1984. Petroleum Formation and Occurrence. Second ed. Springer Verlag, Berlin (699 pp.).
Tyson, R.V., 1993. Palynofacies analysis. In: Jenkins, D.G. (Ed.), Applied Micropaleontology. Kluwer Academic Publishers, Dordrecht, The Netherlands, pp. 153–191.

Tyson, R.V., 1995. Sedimentary Organic Matter: Organic Facies and Palynofacies. Chapman & Hall, London (615 pp.).
Tyson, R.V., 2006. Calibration of hydrogen indices with microscopy: a review, reanalysis and new results using the fluorescence scale. Org. Geochem. 37, 45–63.
Ţabără, D., 2010. Palynology, palynofacies and thermal maturation of the kerogen from the Moldavidian Domain (Gura Humorului area). An. Univ."Al. I. Cuza" Iaşi, Ser. Geol. LVI (2), 53–73.
Ţabără, D., Chirilă, G., 2012. Palaeoclimatic estimation from Miocene of Romania, based on palynological data. Carpath. J. Earth Environ. Sci. 7 (2), 195–208.
Valdés, J., Sifeddine, A., Ortlieb, L., Pierre, C., 2004. Interplay between sedimentary organic matter and dissolved oxygen availability in a coastal zone of the Humboldt Current System; Mejilones Bay, northern Chile. Mar. Geol. 265, 57–166.
van Gijzel, P., 1967. Autofluorescence of fossil pollen and sporeswith special reference to age determination and coalification. Leidse. Geol. Meded. 40, 263–317.
Van Simaeys, S., De Man, E., Vandenberghe, N., Brinkhuis, H., Steurbaut, E., 2004. Stratigraphic and palaeoenvironmental analysis of the Rupelian–Chattian transition in the type region: evidence from dinoflagellate cysts, foraminifera and calcareous nannofossils. Palaeogeogr. Palaeoclimatol. Palaeoecol. 208, 31–58.
Van Simaeys, S., Munsterman, D., Brinkhuis, H., 2005. Oligocene dinoflagellate cyst biostratigraphy of the southern North Sea Basin. Rev. Palaeobot. Palynol. 134, 105–128.
Vandenbroucke, M., 2003. Kerogen: from types to models of chemical structure. Oil Gas Sci. Technol. 58, 243–269.
Vandenbroucke, M., Largeau, C., 2007. Kerogen origin, evolution and structure. Org. Geochem. 38, 719–833.
Wall, D., 1967. Fossil microplankton in deep-sea cores from the Caribbean Sea. Palaeontology 10 (1), 95–123.
Wall, D., Dale, B., Lohmann, G., Smith, W., 1977. The environmental and climatic distribution of dinoflagellate cysts in modern marine sediments from regions in the North and South Atlantic Oceans and adjacent seas. Mar. Micropaleontol. 2, 121–200.
Weiss, H.M., Wilhelms, A., Mills, N., Scotchmer, J., Hall, P.B., Lind, K., Brekke, T., 2000. NIGOGA — The Norwegian Industry Guide to Organic Geochemical Analyses [online]. Edition 4.0 Published by Norsk Hydro, Statoil, Geolab Nor. SINTEF Petroleum Research and the Norwegian Petroleum Directorate (102 pp.).
Williams, G.L., 1978. Palynological biostratigraphy, Deep Sea Drilling Project Sites 367 and 370. In: Lancelot, Y., et al. (Eds.), Deep Sea Drilling Project, Washington, Initial Reports. 41, pp. 783–815.
Williams, G.L., Downie, C., 1966. Further dinoflagellate cysts from the London Clay. In: Davey, R.J., Downie, C., Sarjeant, W.A.S., Williams, G.L. (Eds.), Studies on Mesozoic and Cainozoic Dinoflagellate Cysts. British Museum (Natural History) Geology, Bulletin, Supplement 3, pp. 215–236.
Wilson, L.R., Webster, R.M., 1946. Plant microfossils from a Fort Union coal of Montana. Am. J. Bot. 33, 271–278.
Wood, S.E., Gorin, G.E., 1998. Sedimentary organic matter in distal clinoforms of Miocene slope sediments: site 903 of ODP leg 150, offshore New Jersey (USA). J. Sediment. Res. 68, 856–868.
Zaporozhets, N.I., 1998. Nouvelles données sur la phytostratigraphie d'Eocene et d'Oligocene d'Ergenie du Nord (Sud de la plate-forme russe). Stratigr. Geol. Correl. 6 (3), 56–73 (en russe).
Zonneveld, K.A., Marret, F., Versteegh, G.J., Bogus, K., Bonnet, S., Bouimetarhan, I., Crouch, E., de Vernal, A., Elshanawany, R., Edwards, L., Esper, O., Forke, S., Grøsfjeld, K., Henry, M., Holzwarth, U., Kielt, J.F., Kim, S.Y., Ladouceur, S., Ledu, D., Chen, L., Limoges, A., Londeix, L., Lu, S.H., Mahmoud, M.S., Marino, G., Matsouka, K., Matthiessen, J., Mildenhal, D., Mudie, P., Neil, H., Pospelova, V., Qi, Y., Radi, T., Richerol, T., Rochon, A., Sangiorgi, F., Solignac, S., Turon, J.L., Verleye, T., Wang, Y., Wang, Z., Young, M., 2013. Atlas of modern dinoflagellate cyst distribution based on 2405 data points. Rev. Palaeobot. Palynol. 191, 1–197.